Investigating transcriptional differences in mechanotransductive and ECM related genes in cultured primary corneal keratocytes, fibroblasts and myofibroblasts

Kara Poole[1,*], Krithika S. Iyer[2,3,*], David W. Schmidtke[2,3], W. Matthew Petroll[1,3, †], Victor D. Varner[2,3,†]

[1]Department of Ophthalmology, UT Southwestern Medical Center, Dallas, TX

[2]Department of Bioengineering, University of Texas at Dallas, Richardson, TX

[3]Department of Biomedical Engineering, UT Southwestern Medical Center, Dallas, TX

*****These authors contributed equally to this work

†Corresponding authors

Address correspondence to V.D.V (vdv@utdallas.edu) and W.M.P (matthew.petroll@utsouthwestern.edu

ABSTRACT

After a stromal injury in the cornea, the release of growth factors and pro-inflammatory cytokines typically results in the activation of quiescent keratocytes toward migratory fibroblast and/or fibrotic myofibroblast phenotypes. The persistence of the myofibroblast phenotype can lead to corneal fibrosis and scarring, which are leading causes of blindness worldwide. The primary goal of this study was to establish comprehensive transcriptional profiles for cultured corneal keratocytes, fibroblasts, and myofibroblasts to gain insights into the mechanisms through which changes in phenotype may occur. Here, we cultured primary rabbit corneal keratocytes on collagen-coated glass coverslips in serum free media (SF), serum containing media (FBS), or in the presence of TGF-β1 to induce keratocyte, fibroblast, and myofibroblast phenotypes, respectively. Total RNA was collected and sent to Novogene for bulk RNA sequencing. Subsequent bioinformatic analysis included gene expression quantification, differential expression, and functional analysis. When comparing FBS and TGF-β1 conditions to SF, genes characteristic of a quiescent keratocyte phenotype were downregulated (e.g. KERA, LUM, ALDH1A1), while genes commonly associated with fibroblasts or myofibroblasts were upregulated (e.g. VIM, TNC, FN1, ITGA5, ACTA2). Functional analysis of genes differentially expressed between fibroblasts and keratocytes highlighted pathways related to proliferation (e.g. DNA replication, PI3K-Akt signaling) and cell migration (e.g. Rap1 signaling, ECM-receptor interactions). Enriched pathways for the comparison of myofibroblasts to keratocytes included focal adhesion, regulation of actin cytoskeleton, hippo signaling, and ECM-receptor interaction pathways. Together, these pathways support changes in cytoskeletal organization, cell contractility, mechanotransduction,

and cell-ECM interactions in myofibroblasts compared to keratocytes. Overall, these data demonstrate that there are distinct transcriptional differences between cultured corneal keratocytes, fibroblasts, and myofibroblasts. In our initial analysis, we have identified genes and signaling pathways that may play important roles in keratocyte differentiation, including many related to proliferation, cell mechanical activity, and ECM interactions. Furthermore, our findings reveal novel markers for each cell type as well as possible targets for modulating cell behavior and differentiation to promote physiological corneal wound healing.

INTRODUCTION

The cornea is the soft tissue at the anterior aspect of the eye responsible for bending light towards the retina. It consists of three primary cellular layers: the epithelium, stroma, and endothelium, with the stroma accounting for 90% of the corneal thickness [1–3]. Embedded within the stromal layer, amidst highly aligned collagen lamellae [1,2,4], are the corneal keratocytes [3,5]. In their quiescent state, keratocytes maintain the organized extracellular matrix (ECM) structure [6–8] necessary to retain corneal transparency [9]. However, in response to certain injuries, various growth factors such as transforming growth factor beta-1 (TGF-β1), platelet derived growth factor-BB (PDGF-BB), and fibroblast growth factor (FGF) enter the stromal space and initiate a wound healing response, marked by the transformation of corneal keratocytes from a quiescent, dendritic phenotype into a fibroblastic one [5 10,11]. Consequently, corneal fibroblasts proliferate and migrate towards the site of injury within the stroma [5,12]. Notably, in the presence of a key growth factor, TGF-β1, at the site of injury, fibroblasts further

differentiate towards a fibrotic, myofibroblast phenotype. These cells adopt a spread morphology, express α-smooth muscle actin (α-SMA) and integrate this protein into stress fibers [7,13]. In addition, myofibroblasts contribute to the secretion of a disorganized fibrotic ECM, generate substantial traction forces, and actively participate in the contraction of the injured area [13–19]. Cellular and ECM backscatter during healing can result in corneal haze and a loss of visual acuity.

To replicate these three distinct phenotypes *in vitro*, specific cell culture models have been established: 1) primary corneal keratocytes cultured in defined serum free media to maintain a quiescent phenotype, 2) keratocytes cultured with fetal bovine serum (FBS) to transform them into a fibroblast phenotype, or 3) keratocytes cultured with TGF-β1 to induce a myofibroblast phenotype [20,21]. Utilizing *in vitro* models with these three media conditions, previous studies have investigated the differences in cell morphology, motility [22], and mechanical behavior [19,23–25] between these phenotypes, as well as relative differences in the expression of specific genes and proteins, such as α-SMA. Several of these studies have highlighted the importance of ECM composition, structure and mechanical properties in regulating corneal fibroblast contractility, migration, and ECM reorganization [19,20,24,26,27]. For example, the process of TGF-β1-induced differentiation of myofibroblasts from quiescent keratocytes is highly sensitive to changes in the mechanical stiffness of the ECM [20,25]. However, how keratocytes sense and transduce these external biochemical and mechanical signals to drive changes in differentiation and behavior remains a subject of ongoing research.

Examining global transcriptional patterns could offer novel information on the changes in gene expression associated with keratocyte differentiation into fibroblasts and myofibroblasts. This approach also has the potential to pinpoint novel targets within the associated signaling pathways that precede these phenotypic changes. In this study, we conducted bulk RNA sequencing to establish comprehensive transcriptional profiles for cultured corneal keratocytes (serum free), fibroblasts (FBS) and myofibroblasts (TGF-β1); three cell types that are commonly utilized to mimic *in vivo* quiescent and wound healing phenotypes. The differential gene expression and functional analyses presented here provide insight into the mechanisms through which previously documented changes in phenotype may occur. Of particular interest is the identification of differentially regulated genes and pathways related to mechanical activity and ECM synthesis. In addition, this data set supports the identification of novel markers for each cell type as well as possible targets for modulating cell behavior and differentiation.

METHODS

Isolation and Cell Culture of Primary Rabbit Keratocytes

Primary rabbit corneal keratocytes (NRKs) were isolated from New Zealand white rabbit eyes (Pel-Freez Biologicals, Rogers, AR), and cultured as described previously[21]. Briefly, after removing the epithelium and endothelium, excised corneas were digested in 2.0 mg/mL collagenase (Gibco, Grand Island, NY) and 0.5 mg/mL hyaluronidase (Worthington Biochemical Corporation, Lakewood, NJ) overnight at 37°C. Cells were spun down and plated in 25 cm tissue culture flasks under serum free (SF) conditions. To make SF media, Dulbecco's modified Eagle's medium (DMEM; Sigma-Aldrich, St.

Louis, MO) was supplemented with 100 µM non-essential amino acids (Gibco, Grand Island, NY), 100 µg/mL ascorbic acid (Sigma-Aldrich, St. Louis, MO), 1% RPMI vitamins solution (Sigma-Aldrich, St. Louis, MO), and 1% antibiotic antimycotic solution (Sigma-Aldrich, St. Louis, MO). After 4 days, first passage NRKs were plated at a density of 30,000 cells/mL on unpolymerized collagen-coated substrates in SF media. To produce collagen-coated substrates, untreated 30 mm glass coverslips were incubated with a neutralized solution of 50 µg/mL type I bovine collagen (Advanced BioMatrix, Carlsbad, CA) at 37°C for 30 minutes, then rinsed twice with DMEM[28]. After allowing to attach for 24 hours, cells were cultured in SF media or SF supplemented with 5 ng/mL TGF-β1 (Sigma-Aldrich, St. Louis, MO) for 5 days, or in DMEM containing 10% fetal bovine serum (FBS; Sigma-Aldrich, St. Louis, MO) for 3 days to account for the increased proliferation rate in this condition.

RNA isolation and sequencing

Four samples of total RNA were collected for each treatment condition using the Aurum Total RNA Mini Kit (Bio-Rad, Hercules, CA). Briefly, cells on collagen-coated substrates were washed twice with sterile PBS and lysed using Aurum Total RNA Lysis Solution. The lysate was collected into sterile 1.5 mL tubes and mixed with RNase-Free 70% ethanol before being added to Aurum RNA Binding Mini Columns. A series of centrifugation and low- and high- stringency solution washing steps were performed before eluting the RNA from the columns using molecular biology grade water. The concentration and purity of each sample were confirmed using a Thermo Scientific NanoDrop One[C]. For each treatment condition, two experimental replicates (with four

samples per experiment) were sent to Novogene for bulk RNA-sequencing on Illumina platforms.

Bioinformatic analysis

Initial bioinformatic analysis performed by Novogene included sample and data quality control, mapping to the reference genome (Hisat2 v2.0.5), gene expression quantification (featureCounts v1.5.0-p3), differential expression analysis (DESeq2 R package v1.20.0), and enrichment analysis (clusterProfiler R package v3.8.1). The reference genome utilized for sequence mapping was generated by the McDermott Center Next Generation Sequencing Core at UT Southwestern Medical Center.

Gene Expression Quantification

FPKM (number of Fragments Per Kilobase of transcript sequence per Millions base pairs sequenced) values were calculated based on the length and read count mapped to each gene. FPKM considers the effects of both sequencing depth and gene length and is currently the most common method for estimating gene expression levels. Principal component analysis was performed in MATLAB using FPKM values to observe clustering of samples and treatment groups based on their similarities/differences.

Differential Expression Analysis

Differential expression analysis was performed on the following treatment comparison groups: FBS vs SF, TGF-β1 vs FBS, and TGF-β1 vs SF. Parametric analysis of variance (ANOVA) with Benjamini-Hochberg False Discovery Rate correction at $P = 0.05$ was

performed on normalized data to identify genes that were significantly differentially expressed between treatment groups (adjusted p-value ≤ 0.05 and |log2(Foldchange)| ≥ 1). Heatmaps were created in GraphPad Prism using normalized, log2-transformed FPKM values (log2(FPKM+1)) to display relative expression levels across samples (columns) for sets of differentially expressed genes (DEGs) (rows). Normalized expression levels were calculated by subtracting the values of each row of data from the mean of that row, then diving by the corresponding standard deviation.

Enrichment Analysis

Sets of significant DEGs were further analyzed through Kyoto Encyclopedia of Genes and Genomes (KEGG) enrichment analysis, and pathways with a p-value ≤ 0.05 were considered significantly enriched. Bar plots were generated in GraphPad Prism to visualize pathway significance, the number of up- or downregulated genes associated with each pathway, and the BRITE functional hierarchies under which these pathways are classified. For a subset of the significant KEGG pathways, volcano plots were generated in GraphPad Prism to highlight the fold change and significance of associated genes. A group of genes was chosen for additional analysis of their relative expression and average FPKM values across the three treatment conditions to highlight differences in the transcriptional profiles.

Immunocytochemistry

Additional substrates for each treatment condition were used for F-actin and nuclei labeling and immunostaining for fibronectin, vimentin, or α-SMA to observe cytoskeletal

organization, morphological changes, and the presence of markers commonly associated with each cell type. Cells were fixed in 3% paraformaldehyde in phosphate-buffered saline (PBS) for 10 minutes at room temperature, washed three times in PBS, then permeabilized in 0.5% Triton X-100 in PBS for 15 minutes. Fixed cells were blocked with 1% bovine serum albumin fraction V (Equitech-Bio, Kerrville, TX) in PBS for 1 hour at room temperature. Samples were then incubated with the appropriate primary antibody overnight at 4°C. Fibronectin (A-11) and vimentin (E-5) antibodies were obtained from Santa Cruz Biotechnology (Dallas, TX) and α-SMA (1A4) antibody was obtained from Sigma-Aldrich (St. Louis, MO). After washing three times, samples were incubated with Alexa Fluor 488 conjugated goat anti-mouse secondary antibody and Alexa Fluor 546 Phalloidin (Invitrogen, Waltham, MA) for 2 hours at room temperature, washed, then incubated with 4'-6-diamidino-2-phenylindole (DAPI; Invitrogen, Waltham, MA) for 20 minutes. Confocal microscopy of fixed samples was performed on a Zeiss LSM 800 laser scanning confocal microscope.

Immunoblotting

After rinsing twice with ice-cold, sterile PBS, protein was collected from SF, FBS, and TGF-β1 conditions using a lysis buffer solution containing Pierce RIPA Buffer and Halt Protease & Phosphatase Inhibitor Cocktail (Thermo Scientific; Waltham, MA). Sample lysates were mixed for 30 minutes at 4°C, then centrifuged at 10,000G for 10 minutes at 4°C. Protein concentrations were measured using a Microplate BCA Protein Assay Kit (Thermo Scientific; Waltham, MA) to determine load volumes for 5µg of total protein. Protein samples from SF, FBS, and TGF-β1 conditions were subjected to SDS-PAGE

electrophoresis using Bio-Rad Mini-PROTEAN TGX Gels, then transferred to PVDF membranes (Bio-Rad; Hercules, CA). Membranes were stained for total protein using Ponceau S (Sigma-Aldrich; St. Louis, MO) and subsequently probed with Aldehyde dehydrogenase 1-A1, vimentin (Santa Cruz; Dallas, TX), or α-SMA (Sigma-Aldrich, St. Louis, MO) antibodies followed by an anti-mouse IgG HRP-linked antibody (Cell Signaling; Danvers, MA). Colorimetric (total protein) or chemiluminescence (target protein) imaging was performed using a GE Healthcare Amersham Imager 600 Series. The expression of the target protein was normalized to total protein expression.

Results

Distinct transcriptional differences exist between cells cultured in SF media and in the presence of FBS or TGF-β1.

Principal component analysis (PCA) showed distinct transcriptional differences between corneal keratocytes cultured in either SF medium, FBS-containing medium or medium containing exogenous TGF-β1 (Fig. 1A). PCA is the method of algebraically reducing the dimensionality and extracting significant components from several gene variables to evaluate differences within a group and between different groups in a set of samples[29]. On the PCA map, both technical and experimental replicates within each treatment condition clustered together, while the treatment groups were clearly separated, a result suggestive of distinct gene expression profiles across treatment conditions. Further gene count analysis revealed the number of DEGs between different treatment conditions (Fig. 1B). A comparison of FBS vs. SF contained the highest total number of DEGs at 7693, followed by TGF-β1 vs. FBS at 5704, and TGF-β1 vs. SF at 4430. DEGs

present in more than one comparison are indicated by the overlapping areas within the Venn diagram. 3174 genes were differentially expressed in both FBS- and TGF-β1-treated cells compared to SF conditions, and 1311 genes were differentially expressed across all the treatment groups.

Additionally, there were distinct differences in the number of up- and downregulated DEGs within each comparison (Fig. 1C). Of the total number of DEGs, a greater fraction of genes was downregulated when comparing FBS or TGF-β1 with SF. The heatmap indicates the relative expression of DEGs across all three treatment groups (Fig. 1D). Approximately 50% of these DEGs had high relative expression in SF conditions, while 28% and 22% showed high expression in FBS and TGF-β1 conditions, respectively. The PCA, gene count, and differential expression analysis, thus illustrate distinct and significant differential gene expression patterns between keratocytes cultured in SF media, FBS or TGF-β1.

Markers associated with quiescent keratocytes, fibroblasts, and myofibroblasts are differentially expressed in SF, FBS, and TGF-β1 conditions, respectively.

Our data indicated that genes previously used as markers for corneal keratocytes, fibroblasts, and myofibroblasts were upregulated when treated in SF conditions or with FBS and TGF-β1, respectively. Proteoglycans and crystallins such as keratocan (KERA), mimecan (OGN), decorin (DCN), lumican (LUM), aldehyde dehydrogenase 1 family fember A1 (ALDH1A1) and transketolase (TKT), known to be important for maintaining corneal transparency [2,30,31], were upregulated in SF conditions (Fig. 2A).

Western blot analysis confirmed that this difference in gene expression translates to protein expression as shown by the significant increase in ALDH1A1 when comparing SF to FBS and TGF-β1 treated conditions (Fig. 2B).

Proliferative markers such as marker of proliferation Ki-67 (MKI67) [32,33] and proliferating cell nuclear antigen (PCNA)[34,35] were highly expressed in the presence of FBS compared to SF and TGF-β1 (Fig. 2A). Other markers previously associated with the corneal fibroblast phenotype including vimentin (VIM)[36], a cytoskeletal intermediate filament, and tenascin C (TNC)[37], an ECM protein synthesized in repair tissue, also exhibited elevated expression in FBS treated cells. However, protein expression of vimentin in FBS and TGF-β1 treated conditions did not correspond with the gene expression patterns observed. There was no significant difference in the protein expression levels between FBS and TGF-β1-treated keratocytes (Fig. 2C, S1). This is consistent with previous instances of vimentin also being used as a marker for myofibroblasts[38].

Alpha-smooth muscle actin (α-SMA; ACTA2), which incorporates into stress fibers and plays an important role in the increased contractility of myofibroblasts, is highly expressed in both FBS and TGF-β1-treated conditions (Fig. 2A). In addition to distinct changes in cytoskeletal structure, myofibroblasts also exhibit increased production of ECM proteins present in the fibrotic tissue, including biglycan (BGN)[39] and fibronectin (FN1)[40], both of which are upregulated in TGF-β1-treated conditions. α5β1 integrin (ITGA5, ITGB1), is a common marker for myofibroblast transformation due to its role as

a fibronectin receptor in corneal cells[41]. Our analysis revealed increased expression of ITGA5 in both FBS and TGF-β1-treated conditions, consistent with other studies investigating gene expression in fibroblasts [6,42]. Although the gene expression for certain markers was similar in TGF-β1 and FBS conditions, fibronectin was shown to be almost exclusively present in TGF-β1-treated cells based on both gene expression and immunofluorescent staining (Fig. 2A and 2D).

Overall, our analysis is consistent with existing literature for gene and protein expression patterns associated with three distinct corneal stromal cell phenotypes; SF media supporting a keratocyte phenotype, FBS containing media inducing a fibroblast phenotype, and TGF-β1 inducing a myofibroblast phenotype.

KEGG pathways associated with signal transduction are significantly enriched in the presence of TGF-β1 (myofibroblasts), while pathways associated with genetic information processing are enriched in the presence of FBS (fibroblasts).

KEGG enrichment analysis revealed distinct pathways related to signal transduction and proliferation to be significantly enriched in myofibroblasts and fibroblasts, respectively, compared to quiescent keratocytes (Fig. 3). In the presence of FBS compared to SF, genes were primarily upregulated in pathways related to translation, replication and repair, and cell growth and death. Among these, we saw significant enrichment of the ribosome and ribosome biogenesis pathways, as well as the DNA replication and cell cycle pathways, suggesting a shift towards increased protein synthesis and cell proliferation in FBS conditions (Fig. 3A). In addition, significant

changes in expression were observed for genes involved in the PI3k-Akt and Rap1 signaling pathways and ECM-receptor interactions. These pathways have roles in diverse processes related to proliferation and apoptosis[43–45], adhesion and migration, and cell-cell and cell-matrix interactions[46–49].

Numerous KEGG pathways related to signal transduction, signaling molecules and interaction, and cellular processes, were enriched in the comparison of TGF-β1 treated cells to SF (Fig. 3B). Differential expression of genes within the focal adhesion, regulation of actin cytoskeleton, ECM-receptor interaction, and Rap1 signaling pathways suggest changes in cytoskeletal organization, cell motility and contractility, and cell-ECM interactions in myofibroblasts as compared to keratocytes. Other enriched pathways in this comparison were broadly related to cytokine activity (cytokine-cytokine receptor interaction, TGF-β, JAK-STAT, and TNF signaling pathways) and proliferation/apoptosis (PI3K-Akt, p53, MAPK, and Hippo signaling pathways). Several of these pathways are known to be interconnected or have considerable crosstalk, allowing each pathway to contribute to a range of cellular functions.

When comparing TGF-β1 to FBS treated cells, several of the previously highlighted pathways related to proliferation, cell-ECM interactions, and cytokine activity were enriched (Fig. 3C). However, in contrast to FBS conditions, TGF-β1 treatment resulted in a downregulation of genes within the cell cycle and DNA replication pathways and an upregulation of more genes in the ECM-receptor interaction pathway. An additional pathway related to cell growth and death that was enriched in this comparison was the

cellular senescence KEGG pathway, which has been associated with several biological processes including aging, tumor suppression, and wound healing[50,51]. Taken together, this suggests lower rates of proliferation in TGF-β1 treated cells and a greater emphasis on increased cell-ECM interactions.

Genes related to a proliferative and migratory phenotype are significantly upregulated in fibroblasts.

Within the DNA replication, cell cycle, and PI3K-Akt signaling pathways, genes that support a proliferative phenotype were significantly upregulated in fibroblasts as compared to keratocytes (Fig. 4A-C). An increased expression of several genes that encode for parts of the DNA replication machinery including PCNA, MCM2-7, and several DNA polymerase subunits were found[52]. In fibroblasts, there was an increase in expression of many genes within the PI3K-Akt pathway, such as the receptor tyrosine kinase MET and the MAP Kinase MAP2K1, involved in regulation of proliferation[53,54], and several cyclin dependent kinases (CDKs), which are key regulators of cell cycle progression[55]. The upregulation of genes involved in these selected enriched pathways is supportive of the increased proliferation rate observed in fibroblasts compared to keratocytes and myofibroblasts.

Gene expression indicative of a shift toward a migratory phenotype in fibroblasts was highlighted by changes in the ECM-receptor interaction and Rap1 signaling pathways (Fig. 4D-E). RAP1B encodes for a small GTPase that helps control diverse processes including cell adhesion, migration, and polarity[46,47,56]. Along with increased expression

of RAP1B, there was an upregulation of ACTB (beta actin) which plays a key role in cell motility and migration[57]. A corresponding decrease in focal adhesion related genes like TLN2 (talin) was observed, as well as a decrease in PFN2 (profilin) which is believed to enhance actin polymerization at low concentrations and inhibit it at high concentrations[58]. Changes in ECM-receptor interactions were indicated by changes in the expression of integrins and their corresponding ECM binding partners. This included the downregulation of various collagens (COL1, COL2, COL4, COL6) and the upregulation of TNC (tenascin C), which has been shown to modulate cell adhesion and migration[59,60]. Gene expression was upregulated for several subunits of integrins that allow for cell attachment to tenascin, including ITGA8, ITGAV, ITGB1, and ITGB3. Overall, the observed changes in gene expression for the selected pathways support increased proliferation and cell migration in cultured corneal fibroblasts.

Proliferation related genes are significantly downregulated, while genes involved in cell-ECM interactions and cytokine signaling are upregulated in myofibroblasts compared to fibroblasts.

Several pathways that were enriched in the comparison of fibroblasts to keratocytes were also significantly enriched in the comparison of myofibroblasts to fibroblasts. However, in this comparison, trends in gene expression for the DNA Replication, Cell Cycle, and PI3K-Akt signaling pathways were reversed, indicating lower levels of proliferation in myofibroblasts (Fig. 5A-C). Interestingly, while pro-proliferative genes were downregulated in myofibroblasts as compared to fibroblasts, genes involved in cell cycle arrest and evasion of apoptosis, such as CDKN1A, CDKN2B (cyclin dependent

kinase inhibitor 1A and 2B), and BCL2 (B-cell lymphoma 2) were upregulated (Fig. 5D) [55,61–63].

In contrast to the downregulation of proliferation related genes, there was an upregulation of genes involved in the ECM-receptor interaction pathway (Fig. 5E). Several collagens (COL1A1, COL1A2, COL2A1, COL9A3), fibronectin (FN1), and tenascin N (TNN) were upregulated in myofibroblasts compared to fibroblasts along with some of their associated integrin binding partners (ITGAV, ITGB3)[49,64]. Expression of chondroadherin (CHAD), which has been shown to promote attachment of chondrocytes, fibroblasts, and osteoblasts[65,66], was also significantly upregulated in myofibroblasts. Another interesting gene involved in cell motility, hyaluronan mediated motility receptor (HMMR)[67,68] was downregulated in myofibroblasts compared to fibroblasts.

This comparison also showed significant differences in cytokine expression and signaling (Fig. 5F), including changes in the expression of many TGF-β family genes (Fig. 5G). Several genes that code for secreted ligands of the TGF-β superfamily of proteins were upregulated in myofibroblasts, including growth differentiation factors (GDFs) 6-7 and 9-11 and TGFβ1-3[69]. In addition to inducing myofibroblast transformation, TGF-β1 has been shown to inhibit keratocyte migration and increase collagen synthesis along with TGF-β2[22]. Differences in the roles of fibroblasts and myofibroblasts in corneal inflammatory response may also be reflected by the differential expression of genes encoding for cytokines such as interleukins, IL1A, IL1B

and IL6, and colony stimulating factors, CSF1 and CSF3. These genes were downregulated in myofibroblasts compared to fibroblasts, which are believed to be the cell type responsible for triggering innate immune responses in the cornea[70].

When looking specifically at the TGF-β Signaling Pathway (Fig. 5G), several additional genes stand out as being highly upregulated in myofibroblasts compared to fibroblasts. Two upregulated proteoglycans, decorin (DCN) and fibromodulin (FMOD), known to play a key role in collagen fibril formation were upregulated along with thrombospondin 4 (THBS4), fibrillin 1 (FBN1) and latent transforming growth factor beta binding protein 1 (LTBP1). These genes may help regulate TGF-β activity in myofibroblasts as their encoded proteins can bind and potentially inhibit activated TGF-β[71].

Genes related to ECM interactions and mechanotransduction are differentially regulated in myofibroblasts.

Among the significantly enriched KEGG pathways between myofibroblasts and quiescent keratocytes, the most prominent pathways were associated with ECM interaction and mechanotransduction processes, such as the ECM-receptor interaction, hippo signaling, focal adhesion, regulation of actin cytoskeleton, and TGF-β signaling pathways (Fig. 6). A subset of genes within these pathways along with additional genes of interest were further evaluated for their relative expression across all three treatment conditions (Fig. 7A). At a high level, these genes were classified based on their function and we noticed that a majority of the significantly upregulated genes in myofibroblasts

belonged to families of genes involved in ECM, cell-ECM adhesion, cell-cell interaction, hippo signaling, actomyosin contractility and TGF-β signaling.

Multiple collagens were highly expressed in the myofibroblasts compared to quiescent keratocytes. One of the most notable collagens that was significantly upregulated in myofibroblasts was one which encodes for one of the two alpha chains of type XI collagen, COL11A1 (Collagen type XI alpha 1 chain) (Fig. 7B). Interestingly, several other ECM-related genes, such as TNC (Tenascin-C), SPP1 (Secreted phosphoprotein 1), LRRC15 (Leucine Rich Repeat Containing 15) and IBSP (Integrin binding sialoprotein), and integrins such as ITGA11 (Integrin subunit alpha 11) were also significantly upregulated (Fig. 7B, Table S1). LRRC15 is a membrane protein known to be involved in ECM binding and as a marker for cancer associated myofibroblasts in lung, breast and other tumors [72–74]. Our data revealed a very significant upregulation of LRRC15 in the presence of TGF-β1, compared to cells cultured in serum free conditions. IBSP is a structural bone matrix protein while SPP1 encodes for osteopontin, known to be important in TGF-β1-induced myofibroblast differentiation[75,76] (Fig. 6A, 6C). In the TGF-β signaling pathway, a significant upregulation was observed for TGF-β1 and TGF-β3 in the presence of exogenous TGF-β1 within our in vitro model (Fig. 6E). Within the focal adhesion and regulation of actin cytoskeleton pathways, our data revealed the differential expression of multiple PDGFs (Fig. 6C and 6D). Previous work has suggested that TGF-β1 induces the secretion of PDGF as part of an autocrine signaling loop which regulates myofibroblast differentiation[77]. However, it is still unknown which PDGF subunits are involved in this process. Here, our data shows that

there is a significant upregulation of genes encoding for PDGFA and PDGFC, while PDGFB is downregulated (Fig. 7A).

Furthermore, within the hippo signaling pathway (Fig. 6B), CTGF, which encodes for connective tissue growth factor, and TEA Domain Transcription Factor 4 (TEAD4), were significantly upregulated in myofibroblasts compared to quiescent keratocytes (Fig. 7C). CTGF is a downstream target of YAP activation, a known mechanosensor [78]. Interestingly, TEAD4 was expressed in FBS-treated conditions even more than in TGF-β1 treated conditions. AMOT, encoding for angiomotin, has been known to sequester YAP and TAZ to the cytoplasm, thus reducing the nuclear localization of YAP/TAZ and their downstream effects[79]. Our data indicates that AMOT is significantly downregulated in TGF-β1-treated conditions compared to SF, suggesting nuclear localization of YAP/TAZ. Several genes within the vascular smooth muscle contraction pathway that are involved in actomyosin contractility, such as the myosin light/heavy chains and ACTA2, were also upregulated in myofibroblasts as compared to the quiescent keratocytes (Fig. 6F). ACTA2, a gene encoding for alpha smooth muscle actin (α-SMA), was significantly upregulated in both fibroblasts and myofibroblasts compared to keratocytes (Fig. 7D). α-SMA is an important marker for TGF-β1-induced myofibroblast differentiation[21] and previous studies have shown that the expression of α-SMA in corneal keratocytes is influenced by ECM mechanics[19,23,25].

Another interesting family of genes our data revealed to be differentially expressed in myofibroblasts were the thrombospondins 1,2 and 4 (THBS 1,2,4), known to have the

ability to bind to various ECM proteins and play a key role in cell-ECM and cell-cell interactions [80] (Fig. 7A). THBS1 specifically, was significantly upregulated in the myofibroblasts compared to the quiescent keratocytes (Fig. 7D) and is known to be important for TGF-β1-induced myofibroblast differentiation[81].

Discussion

While many phenotypic differences between corneal keratocytes, fibroblasts, and myofibroblasts have been well documented both *in vivo* and *in vitro*, the transcriptional changes and signaling pathways regulating these differences remain a subject of ongoing research. Improving our understanding of keratocyte differentiation from a genomic perspective could have important implications in corneal wound healing and fibrosis. For this study, we utilized a 2D *in vitro* model in which corneal keratocytes are cultured in serum free media (SF), serum containing media (FBS), or SF with TGF-β1 to produce corneal keratocytes, fibroblasts, and myofibroblasts, respectively. We then performed bulk RNA sequencing to obtain a global view of the transcriptional differences between cells in these three treatment conditions. The differential gene expression and functional analyses presented here not only provide insight into the mechanisms underlying the phenotypic changes observed in previous studies, but also support the identification of novel markers for each cell type as well as potential targets for modulating cell behavior and differentiation.

Previous studies have documented several key phenotypic differences between keratocytes, fibroblasts, and myofibroblasts. These include changes in proliferation, ECM synthesis, morphology/cytoskeletal organization, and mechanical activity (adhesion, migration/motility, contractility/force generation) [7,12,20,21,23,25,82–85]. Our analysis revealed unique gene expression profiles that likely support these differences, as many of the DEGs and enriched signaling pathways were related to proliferation, ECM, and cell mechanics. Within these pathways, we also identified several DEGs that may warrant further investigation to determine their functional significance in the transformation of keratocytes into fibroblasts and myofibroblasts.

The transformation of quiescent keratocytes to a proliferative and migratory fibroblastic phenotype is an integral step in the process of corneal wound healing following injury or surgery[22,86]. Our results suggest that the increased proliferation observed in corneal fibroblasts is associated with the upregulation of genes involved in the DNA replication, cell cycle, and PI3K-Akt signaling pathways. This proliferative gene expression signature in fibroblasts includes the upregulation of key genes such as E2F1/2 and CDK2/4/6 as compared to keratocytes and myofibroblasts. These genes and their associated signaling pathways may be of further interest as targets for accelerating the repopulation of a decellularized wound area, or in the pursuit of stromal regeneration[87].

The presence of myofibroblasts is important for wound closure, however, their persistence can lead to unwanted fibrosis[86,88]. In our analysis, while genes associated with proliferation were downregulated, the myofibroblasts appear to take on a similar

apoptotic-resistant phenotype that is seen in pathological wound healing responses[89,90], as indicated by changes in the cell cycle, cellular senescence, PI3K-Akt, and p53 signaling pathways. Genes within these pathways that may be of particular interest include BCL2 (upregulated in myofibroblasts compared to both keratocytes and fibroblasts), which is known to be capable of blocking apoptosis and has been a target of interest for various cancer types and in wound repair[63,91,92]. In general, the evasion of apoptosis by myofibroblasts is considered a hallmark of fibrotic disease, making therapeutic modulation of the cell cycle and apoptosis of interest in a range of pathologies[89,93,94]. In the case of corneal wound healing, targeting genes related to apoptosis could be used to support the timely disappearance of myofibroblasts after wound closure to help prevent a fibrotic response.

The synthesis and degradation of ECM proteins by keratocytes is important for maintaining the stromal composition and structure that allows for corneal transparency. This ECM maintenance phenotype is disrupted in the transformation of keratocytes to fibroblasts and myofibroblasts, due to changes in the types and quantities of ECM proteins being produced. Although previous work has identified several collagens and proteoglycans that are differentially expressed between these corneal cell types, the data obtained in this study provides more comprehensive ECM gene expression signatures as we are able to look at the entire “matrisome” [95,96]. The matrisome includes core ECM proteins (e.g. collagens, proteoglycans, glycoproteins), cellular receptors for ECM (e.g. integrins), ECM-modifying enzymes, and ECM-binding growth factors/cytokines. Altered expression of genes encoding for these proteins can result in

changes to matrix composition and structure and can impact a wide range of cellular processes from proliferation to cytoskeletal organization and mechanical activity.

How the myofibroblast matrisome differs from that of keratocytes and fibroblasts is of particular interest in this study because a key component of the myofibroblast phenotype is the synthesis of an unorganized, fibrotic ECM. Our data supports previous findings that gene expression for proteoglycans produced by keratocytes to regulate stromal collagen organization (e.g. KERA, OGN, DCN) is reduced in myofibroblasts, while gene expression for ECM proteins associated with fibrosis (e.g. COL3A1, FN1) is enriched [40]. Our analysis revealed many additional ECM-related genes that were highly upregulated in myofibroblasts and may contribute to their fibrotic phenotype, including osteopontin (SPP1 or OPN), and integrin binding sialoprotein (IBSP). Each of these genes are primarily expressed in bone matrix, but there is also evidence supporting their roles in wound healing and fibrosis [75,76 97–101]. Osteopontin has been shown to be important in TGF-β1-induced myofibroblast differentiation in dermal and cardiac fibroblasts and is believed to be a promising therapeutic target in cardiac fibrosis. In the cornea, an osteopontin KO mouse displayed delayed wound healing after incisional injury that corresponded to lower levels of TGF-β1 expression and fewer myofibroblasts [99].

Alterations in ECM composition during wound healing elicits changes in cellular behavior through interactions with cell membrane receptors. Tenascin C (TNC) and fibronectin (FN1), which in this study were highly expressed in fibroblasts and

myofibroblasts, respectively, have been investigated extensively due to their roles in inflammation, wound healing, and tissue remodeling [86,101,102]. Tenascin C modulates cellular adhesion and migration through several integrin receptors (α8β1, α9β1, α7β1), which also showed enhanced gene expression in fibroblasts. The increase in TNC and changes in integrin expression work together to support the anti-adhesive and pro-migratory phenotype of fibroblasts, that along with proliferation, is critical in the early response to corneal injury. In contrast to tenascin C, fibronectin is a major adhesive ECM component. Along with increased expression of fibronectin, changes in the types and localization of focal adhesion proteins have been previously documented for myofibroblasts[25,84]. Our study saw the upregulation of many genes encoding for focal adhesion components in myofibroblasts, such as vinculin (VCL), talin (TLN2), and paxillin (PXN). The development of mature focal adhesions plays an important role in the distinct mechanical phenotype of myofibroblasts, including their increased contractility and the generation of greater traction forces on the surrounding ECM[84].

The comparisons made in this study help to identify distinct ECM-related gene expression signatures for keratocytes, fibroblasts, and myofibroblasts that contribute to their associated phenotypes. ECM gene expression patterns in keratocytes promote a quiescent, ECM maintenance phenotype, while altered gene expression promotes a migratory phenotype in fibroblasts and a fibrotic and contractile phenotype in myofibroblasts. How ECM composition and cell-ECM interactions change throughout the corneal wound healing process remains a topic of great interest due to the importance of ECM structure and composition in regaining corneal transparency.

In vitro experiments, particularly those employing three-dimensional collagen matrices, have also highlighted the importance of ECM mechanics and stiffness in regulating corneal cell migration, contractility, and ECM reorganization [19,20,24,26,27]. Furthermore, the process of TGF-β1-induced differentiation of myofibroblasts from quiescent keratocytes is highly sensitive to changes in the mechanical properties of the ECM [20,25]. In the presence of TGF-β1, keratocytes cultured on softer, uncompressed 3D collagen gels, exhibit fewer stress fibers and reduced expression of α-SMA compared to cells cultured on stiffer, more compressed collagen matrices [14,19,82,83,103,104]. Other in vitro studies using polyacrylamide gels of varying stiffnesses have shown that corneal keratocytes cultured on stiffer substrata exhibit elevated levels of myofibroblast differentiation in response to TGF-β1, as indicated by an increased number of α-SMA positive cells. This elevated differentiation is also accompanied by changes in the contractile behavior of the cells and the arrangement of focal adhesions at the subcellular level [25,84].

Given that the stiffness of the extracellular matrix (ECM) is recognized as a significant factor in myofibroblast differentiation, we speculated that mechanotransduction-related genes and signaling pathways would be upregulated following culture in the presence of TGF-β1. Our results identified enrichment of pathways related to cell contractility (smooth muscle contraction pathway) and mechanotransduction (hippo pathway) that include several genes that may contribute to the mechanical differences observed between myofibroblasts and keratocytes. Genes in the hippo pathway that could be

contributing to this difference in mechanosensitivity between keratocytes and myofibroblasts include changes in the expression of AMOT and SMADs that coordinate the localization of YAP/TAZ in myofibroblasts. YAP and TAZ have previously been reported to help regulate myofibroblast differentiation in human corneal fibroblasts[105]. AMOT, the gene encoding for angiomotin, binds to YAP and TAZ and sequesters them in the cytoplasm. In our study, the downregulation of AMOT suggests that YAP/TAZ are able to translocate to the nucleus and interact with various transcription factors. This idea is supported by the increased expression of CTGF, a downstream target of YAP activation [78], that is seen in
myofibroblasts as compared to keratocytes. Note that the expression of CTGF is reduced when AMOT is overexpressed [79].

Within the smooth muscle contraction pathway, ACTA2, the gene encoding for alpha smooth muscle actin, was significantly upregulated in myofibroblasts compared to keratocytes. This is an important marker of myofibroblast transformation, and the incorporation of α-SMA into stress fibers has been shown to play a significant role in the increased contractility and force generation in these cells[13]. Interestingly, even higher expression of the ACTA2 gene was found in our fibroblast condition, although incorporation of α-SMA into stress fibers was not observed by immunostaining (Fig. S2A). We chose the 5-day time point for our TGF-β1 culture model because we wanted to study the mature myofibroblast phenotype that is associated with corneal fibrosis. In serum containing media however, RNA was isolated after 3 days of culture as cells transform sooner and become confluent at later time points due to the increased

proliferation. Based on previous experiments, we know that there is abundant protein expression of α-SMA after 5 days of culture in TGF-β1, but the peak in gene expression may be happening sooner, thereby explaining the higher expression of ACTA2 in fibroblasts. This is supported by our western blotting results showing much lower expression of alpha-SMA protein in fibroblasts, despite the higher gene expression level (Fig. S2B). Furthermore, an increase in mRNA expression does not always correlate with protein expression due to post-translational regulation.

As a whole, our findings using bulk RNA sequencing provide the first comprehensive differential gene expression profile for cultured corneal keratocytes, fibroblasts, and myofibroblasts. In our initial analysis, we have identified genes and signaling pathways that may play important roles in keratocyte differentiation and the maintenance of keratocyte, fibroblast, and myofibroblast phenotypes. In the future, this sequencing data set can continue to be a resource to identify potential targets for guiding keratocyte differentiation and behavior and serve as a foundation for future studies investigating the influence of substratum stiffness on corneal keratocyte gene expression. Additional experiments targeting specific genes of interest can further reveal the biological and functional significance of these findings as they relate to the broader fields of wound healing, fibrosis, and tissue engineering.

AUTHOR CONTRIBUTIONS

KP, KSI, VDV, WMP, and DWS conceived the study and designed experiments. KSI and KP conducted all experiments and analyzed all experimental data. All authors discussed

and interpreted results. KP, KSI, VDV, and WMP wrote the manuscript with feedback from all authors.

FUNDING

This work was supported by the NIH grants R01 EY013322, R01 EY030190, and P30 EY030413, as well as a Challenge grant from Research to Prevent Blindness.

ACKNOWLEDGMENTS

We would also like to thank the members of the Varner, Petroll, and Schmidtke labs for their many helpful discussions and comments.

REFERENCES

1. Meek KM, Boote C. The use of X-ray scattering techniques to quantify the orientation and distribution of collagen in the corneal stroma. *Prog Retin Eye Res*. 2009;28(5):369-392. doi:10.1016/j.preteyeres.2009.06.005

2. Meek KM. Corneal collagen—its role in maintaining corneal shape and transparency. *Biophysical Rev*. 2009;1(2):83-93. doi:10.1007/s12551-009-0011-x

3. Nishida T, Yasumoto K, Otori T, Desaki J. The network structure of corneal fibroblasts in the rat as revealed by scanning electron microscopy. *Invest Ophth Vis Sci*. 1988;29(12):1887-1890.

4. Worthen DM. Histology of the Human Eye. *Arch Ophthalmol*. 1972;88(2):234-234. doi:10.1001/archopht.1972.01000030236034

5. Fini ME. Keratocyte and fibroblast phenotypes in the repairing cornea. *Prog Retin Eye Res*. 1999;18(4):529-551. doi:10.1016/s1350-9462(98)00033-0

6. Beales MP, Funderburgh JL, Jester JV, Hassell JR. Proteoglycan synthesis by bovine keratocytes and corneal fibroblasts: maintenance of the keratocyte phenotype in culture. *Investig Ophthalmol Vis Sci*. 1999;40(8):1658-1663.

7. Jester JV, Barry PA, Lind GJ, Petroll WM, Garana R, Cavanagh HD. Corneal keratocytes: in situ and in vitro organization of cytoskeletal contractile proteins. *Investig Ophthalmol Vis Sci*. 1994;35(2):730-743.

8. Zieske JD, Guimarães SR, Hutcheon AEK. Kinetics of Keratocyte Proliferation in Response to Epithelial Debridement. *Exp Eye Res*. 2001;72(1):33-39. doi:10.1006/exer.2000.0926

9. Hassell JR, Birk DE. The molecular basis of corneal transparency. *Exp Eye Res*. 2010;91(3):326-335. doi:10.1016/j.exer.2010.06.021

10. Imanishi J, Kamiyama K, Iguchi I, Kita M, Sotozono C, Kinoshita S. Growth factors: importance in wound healing and maintenance of transparency of the cornea. *Prog Retin Eye Res*. 2000;19(1):113-129. doi:10.1016/s1350-9462(99)00007-5

11. Wilson SE, Mohan RR, Mohan RR, Ambrósio R, Hong J, Lee J. The Corneal Wound Healing Response: Cytokine-mediated Interaction of the Epithelium, Stroma, and Inflammatory Cells. *Prog Retin Eye Res*. 2001;20(5):625-637. doi:10.1016/s1350-9462(01)00008-8

12. Petroll WM, Kivanany PB, Hagenasr D, Graham EK. Corneal Fibroblast Migration Patterns During Intrastromal Wound Healing Correlate With ECM Structure and Alignment. *Investig Opthalmology Vis Sci*. 2015;56(12):7352. doi:10.1167/iovs.15-17978

13. Jester JV, Petroll WM, Barry PA, Cavanagh HD. Expression of alpha-smooth muscle (alpha-SM) actin during corneal stromal wound healing. *Investig Ophthalmol Vis Sci*. 1995;36(5):809-819.

14. Jester JV, Ho-Chang J. Modulation of cultured corneal keratocyte phenotype by growth factors/cytokines control in vitro contractility and extracellular matrix contraction. *Exp Eye Res*. 2003;77(5):581-592. doi:10.1016/s0014-4835(03)00188-x

15. Myrna KE, Pot SA, Murphy CJ. Meet the corneal myofibroblast: the role of myofibroblast transformation in corneal wound healing and pathology. *Vet Ophthalmol*. 2009;12:25-27. doi:10.1111/j.1463-5224.2009.00742.x

16. Nakamura K. Interaction Between Injured Corneal Epithelial Cells and Stromal Cells. *Cornea*. 2003;22(7):S35-S47. doi:10.1097/00003226-200310001-00006

17. Kurosaka H, Kurosaka D, Kato K, Mashima Y, Tanaka Y. Transforming growth factor-beta 1 promotes contraction of collagen gel by bovine corneal fibroblasts through differentiation of myofibroblasts. *Investig Ophthalmol Vis Sci*. 1998;39(5):699-704.

18. Jester JV, Huang J, Barry-Lane PA, Kao WW, Petroll WM, Cavanagh HD. Transforming growth factor(beta)-mediated corneal myofibroblast differentiation requires actin and fibronectin assembly. *Investig Ophthalmol Vis Sci*. 1999;40(9):1959-1967.

19. Petroll WM, Miron-Mendoza M. Mechanical interactions and crosstalk between corneal keratocytes and the extracellular matrix. *Exp Eye Res*. 2015;133:49-57. doi:10.1016/j.exer.2014.09.003

20. Kim A, Lakshman N, Karamichos D, Petroll WM. Growth Factor Regulation of Corneal Keratocyte Differentiation and Migration in Compressed Collagen Matrices. *Investig Opthalmology Vis Sci*. 2010;51(2):864. doi:10.1167/iovs.09-4200

21. Jester JV, Barry-Lane PA, Cavanagh HD, Petroll WM. Induction of α-Smooth Muscle Actin Expression and Myofibroblast Transformation in Cultured Corneal Keratocytes. *Cornea*. 1996;15(5):505-516. doi:10.1097/00003226-199609000-00011

22. Andresen JL, Ledet T, Ehlers N. Keratocyte migration and peptide growth factors: the effect of PDGF, bFGF, EGF, IGF-I, aFGF and TGF-ß on human keratocyte migration in a collagen gel. *Curr Eye Res*. 1997;16(6):605-613. doi:10.1076/ceyr.16.6.605.5081

23. Lakshman N, Petroll WM. Growth factor regulation of corneal keratocyte mechanical phenotypes in 3-D collagen matrices. *Investig Ophthalmol Vis Sci*. 2012;53(3):1077-1086. doi:10.1167/iovs.11-8609

24. Kim A, Zhou C, Lakshman N, Petroll WM. Corneal stromal cells use both high- and low-contractility migration mechanisms in 3-D collagen matrices. *Exp Cell Res*. 2012;318(6):741-752. doi:10.1016/j.yexcr.2011.12.018

25. Maruri DP, Miron-Mendoza M, Kivanany PB, et al. ECM Stiffness Controls the Activation and Contractility of Corneal Keratocytes in Response to TGF-β1. *Biophys J*. 2020;119(9):1865-1877. doi:10.1016/j.bpj.2020.08.040

26. Kim A, Lakshman N, Petroll WM. Quantitative assessment of local collagen matrix remodeling in 3-D Culture: The role of Rho kinase. *Exp Cell Res*. 2006;312(18):3683-3692. doi:10.1016/j.yexcr.2006.08.009

27. Miron-Mendoza M, Graham E, Kivanany P, Quiring J, Petroll WM. The Role of Thrombin and Cell Contractility in Regulating Clustering and Collective Migration of Corneal Fibroblasts in Different ECM Environments. *Investig Opthalmology Vis Sci*. 2015;56(3):2079. doi:10.1167/iovs.15-16388

28. Kivanany PB, Grose KC, Yonet-Tanyeri N, et al. An In Vitro Model for Assessing Corneal Keratocyte Spreading and Migration on Aligned Fibrillar Collagen. *J Funct Biomaterials*. 2018;9(4):54. doi:10.3390/jfb9040054

29. Ringnér M. What is principal component analysis? *Nat Biotechnol*. 2008;26(3):303-304. doi:10.1038/nbt0308-303

30. Hassell JR, Cintron C, Kublin C, Newsome DA. Proteoglycan changes during restoration of transparency in corneal scars. *Arch Biochem Biophys*. 1983;222(2):362-369. doi:10.1016/0003-9861(83)90532-5

31. Jester JV. Corneal crystallins and the development of cellular transparency. *Semin Cell Dev Biol*. 2008;19(2):82-93. doi:10.1016/j.semcdb.2007.09.015

32. McKay TB, Hutcheon AEK, Zieske JD, Ciolino JB. Extracellular Vesicles Secreted by Corneal Epithelial Cells Promote Myofibroblast Differentiation. *Cells*. 2020;9(5):1080. doi:10.3390/cells9051080

33. Dong Z, Zhou X, Wu J, et al. Small incision lenticule extraction (SMILE) and femtosecond laser LASIK: comparison of corneal wound healing and inflammation. *Br J Ophthalmol*. 2014;98(2):263. doi:10.1136/bjophthalmol-2013-303415

34. Yusoff NZ binte M, Riau AK, Yam GHF, Halim NSH binte, Mehta JS. Isolation and Propagation of Human Corneal Stromal Keratocytes for Tissue Engineering and Cell Therapy. *Cells*. 2022;11(1):178. doi:10.3390/cells11010178

35. Gan L, Fagerholm P, Ekenbark S. Expression of proliferating cell nuclear antigen in corneas kept in long term culture. *Acta Ophthalmol Scand*. 1998;76(3):308-313. doi:10.1034/j.1600-0420.1998.760311.x

36. Wilson SE. The Yin and Yang of Mesenchymal Cells in the Corneal Stromal Fibrosis Response to Injury: The Cornea as a Model of Fibrosis in Other Organs. *Biomolecules*. 2022;13(1):87. doi:10.3390/biom13010087

37. Latvala T, Tervo K, Mustonen R, Tervo T. Expression of cellular fibronectin and tenascin in the rabbit cornea after excimer laser photorefractive keratectomy: a 12 month study. *Br J Ophthalmol*. 1995;79(1):65. doi:10.1136/bjo.79.1.65

38. Chaurasia SS, Kaur H, Medeiros FW de, Smith SD, Wilson SE. Dynamics of the expression of intermediate filaments vimentin and desmin during myofibroblast differentiation after corneal injury. *Exp Eye Res*. 2009;89(2):133-139. doi:10.1016/j.exer.2009.02.022

39. Funderburgh JL, Funderburgh ML, Mann MM, Corpuz L, Roth MR. Proteoglycan Expression during Transforming Growth Factor β-induced Keratocyte-Myofibroblast

Transdifferentiation*. *J Biol Chem*. 2001;276(47):44173-44178. doi:10.1074/jbc.m107596200

40. Garana RM, Petroll WM, Chen WT, et al. Radial keratotomy. II. Role of the myofibroblast in corneal wound contraction. *Investig Ophthalmol Vis Sci*. 1992;33(12):3271-3282.

41. Welch MP, Odland GF, Clark RA. Temporal relationships of F-actin bundle formation, collagen and fibronectin matrix assembly, and fibronectin receptor expression to wound contraction. *J cell Biol*. 1990;110(1):133-145. doi:10.1083/jcb.110.1.133

42. Masur SK, Cheung JK, Antohi S. Identification of integrins in cultured corneal fibroblasts and in isolated keratocytes. *Investig Ophthalmol Vis Sci*. 1993;34(9):2690-2698.

43. Engelman JA, Luo J, Cantley LC. The evolution of phosphatidylinositol 3-kinases as regulators of growth and metabolism. *Nat Rev Genet*. 2006;7(8):606-619. doi:10.1038/nrg1879

44. Kim DH, Chung JK. Akt: Versatile Mediator of Cell Survival and Beyond. *BMB Rep*. 2002;35(1):106-115. doi:10.5483/bmbrep.2002.35.1.106

45. Chen K, Li Y, Zhang X, Ullah R, Tong J, Shen Y. The role of the PI3K/AKT signalling pathway in the corneal epithelium: recent updates. *Cell Death Dis*. 2022;13(5):513. doi:10.1038/s41419-022-04963-x

46. Bos JL. Linking Rap to cell adhesion. *Curr Opin Cell Biol*. 2005;17(2):123-128. doi:10.1016/j.ceb.2005.02.009

47. Boettner B, Aelst LV. Control of cell adhesion dynamics by Rap1 signaling. *Curr Opin Cell Biol*. 2009;21(5):684-693. doi:10.1016/j.ceb.2009.06.004

48. Bosman FT, Stamenkovic I. Functional structure and composition of the extracellular matrix. *J Pathol*. 2003;200(4):423-428. doi:10.1002/path.1437

49. Flier A van der, Sonnenberg A. Function and interactions of integrins. *Cell Tissue Res*. 2001;305(3):285-298. doi:10.1007/s004410100417

50. Childs BG, Durik M, Baker DJ, Deursen JM van. Cellular senescence in aging and age-related disease: from mechanisms to therapy. *Nat Med*. 2015;21(12):1424-1435. doi:10.1038/nm.4000

51. Muñoz-Espín D, Serrano M. Cellular senescence: from physiology to pathology. *Nat Rev Mol Cell Biol*. 2014;15(7):482-496. doi:10.1038/nrm3823

52. Waga S, Stillman B. THE DNA REPLICATION FORK IN EUKARYOTIC CELLS. *Biochemistry*. 1998;67(1):721-751. doi:10.1146/annurev.biochem.67.1.721

53. Trusolino L, Bertotti A, Comoglio PM. MET signalling: principles and functions in development, organ regeneration and cancer. *Nat Rev Mol Cell Biol*. 2010;11(12):834-848. doi:10.1038/nrm3012

54. Organ SL, Tsao MS. An overview of the c-MET signaling pathway. *Ther Adv Méd Oncol*. 2011;3(1_suppl):S7-S19. doi:10.1177/1758834011422556

55. Łukasik P, Załuski M, Gutowska I. Cyclin-Dependent Kinases (CDK) and Their Role in Diseases Development–Review. *Int J Mol Sci*. 2021;22(6):2935. doi:10.3390/ijms22062935

56. Wilson JM, Prokop JW, Lorimer E, Ntantie E, Williams CL. Differences in the Phosphorylation-Dependent Regulation of Prenylation of Rap1A and Rap1B. *J Mol Biol*. 2016;428(24):4929-4945. doi:10.1016/j.jmb.2016.10.016

57. Bunnell TM, Burbach BJ, Shimizu Y, Ervasti JM. β-Actin specifically controls cell growth, migration, and the G-actin pool. *Mol Biol Cell*. 2011;22(21):4047-4058. doi:10.1091/mbc.e11-06-0582

58. Ding Z, Roy P. Profilin-1 versus profilin-2: two faces of the same coin? *Breast Cancer Res*. 2013;15(3):311. doi:10.1186/bcr3433

59. Jones FS, Jones PL. The tenascin family of ECM glycoproteins: Structure, function, and regulation during embryonic development and tissue remodeling. *Dev Dyn*. 2000;218(2):235-259. doi:10.1002/(sici)1097-0177(200006)218:2<235::aid-dvdy2>3.0.co;2-g

60. Midwood KS, Orend G. The role of tenascin□C in tissue injury and tumorigenesis. *J Cell Commun Signal*. 2009;3(3-4):287-310. doi:10.1007/s12079-009-0075-1

61. Bartkova J, Grøn B, Dabelsteen E, Bartek J. Cell-cycle regulatory proteins in human wound healing. *Arch Oral Biol*. 2003;48(2):125-132. doi:10.1016/s0003-9969(02)00202-9

62. Reed J. Bcl-2 and the regulation of programmed cell death. *J cell Biol*. 1994;124(1):1-6. doi:10.1083/jcb.124.1.1

63. Ruvolo P, Deng X, May W. Phosphorylation of Bcl2 and regulation of apoptosis. *Leukemia*. 2001;15(4):515-522. doi:10.1038/sj.leu.2402090

64. Degen M, Brellier F, Kain R, et al. Tenascin-W Is a Novel Marker for Activated Tumor Stroma in Low-grade Human Breast Cancer and Influences Cell Behavior. *Cancer Res*. 2007;67(19):9169-9179. doi:10.1158/0008-5472.can-07-0666

65. Mizuno M, Fujisawa R, Kuboki Y. Bone chondroadherin promotes attachment of osteoblastic cells to solid-state substrates and shows affinity to collagen. *Calcif Tissue Int*. 1996;59(3):163-167. doi:10.1007/s002239900103

66. Camper L, Heinegård D, Lundgren-□kerlund E. Integrin α2β1 Is a Receptor for the Cartilage Matrix Protein Chondroadherin. *J Cell Biol*. 1997;138(5):1159-1167. doi:10.1083/jcb.138.5.1159

67. Tolg C, McCarthy JB, Yazdani A, Turley EA. Hyaluronan and RHAMM in Wound Repair and the "Cancerization" of Stromal Tissues. *BioMed Res Int*. 2014;2014:103923. doi:10.1155/2014/103923

68. Hinneh JA, Gillis JL, Moore NL, Butler LM, Centenera MM. The role of RHAMM in cancer: Exposing novel therapeutic vulnerabilities. *Front Oncol*. 2022;12:982231. doi:10.3389/fonc.2022.982231

69. Wrana JL. Signaling by the TGFβ Superfamily. *Cold Spring Harb Perspect Biol*. 2013;5(10):a011197. doi:10.1101/cshperspect.a011197

70. Fukuda K. Corneal fibroblasts: Function and markers. *Exp Eye Res*. 2020;200:108229. doi:10.1016/j.exer.2020.108229

71. Soo C, Hu FY, Zhang X, et al. Differential Expression of Fibromodulin, a Transforming Growth Factor-β Modulator, in Fetal Skin Development and Scarless Repair. *Am J Pathol*. 2000;157(2):423-433. doi:10.1016/s0002-9440(10)64555-5

72. Purcell JW, Tanlimco SG, Hickson J, et al. LRRC15 Is a Novel Mesenchymal Protein and Stromal Target for Antibody–Drug Conjugates. *Cancer Res*. 2018;78(14):4059-4072. doi:10.1158/0008-5472.can-18-0327

73. Krishnamurty AT, Shyer JA, Thai M, et al. LRRC15+ myofibroblasts dictate the stromal setpoint to suppress tumour immunity. *Nature*. 2022;611(7934):148-154. doi:10.1038/s41586-022-05272-1

74. Krishnamurty A, Shyer J, Thai M, et al. 1434 TGFβ-dependent LRRC15 + myofibroblasts dictate the tumor fibroblast setpoint to promote cancer immunotherapy resistance. *Regul Young Investig Award Abstr*. Published online 2023:A1597-A1597. doi:10.1136/jitc-2023-sitc2023.1434

75. Lenga Y, Koh A, Perera AS, McCulloch CA, Sodek J, Zohar R. Osteopontin Expression Is Required for Myofibroblast Differentiation. *Circ Res*. 2008;102(3):319-327. doi:10.1161/circresaha.107.160408

76. Mohamed IA, Gadeau AP, Hasan A, Abdulrahman N, Mraiche F. Osteopontin: A Promising Therapeutic Target in Cardiac Fibrosis. *Cells*. 2019;8(12):1558. doi:10.3390/cells8121558

77. Jester JV, Huang J, Petroll WM, Cavanagh HD. TGFβ Induced Myofibroblast Differentiation of Rabbit Keratocytes Requires Synergistic TGFβ, PDGF and Integrin Signaling. *Exp Eye Res*. 2002;75(6):645-657. doi:10.1006/exer.2002.2066

78. Raghunathan VK, Dreier B, Morgan JT, et al. Involvement of YAP, TAZ and HSP90 in Contact Guidance and Intercellular Junction Formation in Corneal Epithelial Cells. *PLoS ONE*. 2014;9(10):e109811. doi:10.1371/journal.pone.0109811

79. Chan SW, Lim CJ, Chong YF, Pobbati AV, Huang C, Hong W. Hippo Pathway-independent Restriction of TAZ and YAP by Angiomotin*. *J Biol Chem*. 2011;286(9):7018-7026. doi:10.1074/jbc.c110.212621

80. Lahav J. The functions of thrombospondin and its involvement in physiology and pathophysiology. *Biochim Biophys Acta (BBA) - Mol Basis Dis*. 1993;1182(1):1-14. doi:10.1016/0925-4439(93)90146-r

81. Bradshaw AD. Principles of Tissue Engineering (Fourth Edition). *Part 2: Vitr Control Tissue Dev*. Published online 2014:279-290. doi:10.1016/b978-0-12-398358-9.00015-x

82. Lakshman N, Kim A, Petroll WM. Characterization of corneal keratocyte morphology and mechanical activity within 3-D collagen matrices. *Exp Eye Res*. 2010;90(2):350-359. doi:10.1016/j.exer.2009.11.016

83. Karamichos D, Lakshman N, Petroll WM. Regulation of corneal fibroblast morphology and collagen reorganization by extracellular matrix mechanical properties. *Investig Ophthalmol Vis Sci*. 2007;48(11):5030-5037. doi:10.1167/iovs.07-0443

84. Maruri DP, Iyer KS, Schmidtke DW, Petroll WM, Varner VD. Signaling Downstream of Focal Adhesions Regulates Stiffness-Dependent Differences in the TGF-β1-Mediated Myofibroblast Differentiation of Corneal Keratocytes. *Front Cell Dev Biol*. 2022;10:886759. doi:10.3389/fcell.2022.886759

85. Iyer KS, Maruri DP, Peak KE, Schmidtke DW, Petroll WM, Varner VD. ECM stiffness modulates the proliferation but not the motility of primary corneal keratocytes in response to PDGF-BB. *Exp Eye Res*. 2022;220:109112. doi:10.1016/j.exer.2022.109112

86. Kamil S, Mohan RR. Corneal stromal wound healing: Major regulators and therapeutic targets. *Ocul Surf*. 2021;19:290-306. doi:10.1016/j.jtos.2020.10.006

87. Lagali N. Corneal Stromal Regeneration: Current Status and Future Therapeutic Potential. *Curr Eye Res*. 2020;45(3):278-290. doi:10.1080/02713683.2019.1663874

88. Desai VD, Hsia HC, Schwarzbauer JE. Reversible Modulation of Myofibroblast Differentiation in Adipose-Derived Mesenchymal Stem Cells. *PLoS ONE*. 2014;9(1):e86865. doi:10.1371/journal.pone.0086865

89. Hinz B, Lagares D. Evasion of apoptosis by myofibroblasts: a hallmark of fibrotic diseases. *Nat Rev Rheumatol*. 2020;16(1):11-31. doi:10.1038/s41584-019-0324-5

90. McElhinney K, Irnaten M, O'Brien C. p53 and Myofibroblast Apoptosis in Organ Fibrosis. *Int J Mol Sci*. 2023;24(7):6737. doi:10.3390/ijms24076737

91. Qian S, Wei Z, Yang W, Huang J, Yang Y, Wang J. The role of BCL-2 family proteins in regulating apoptosis and cancer therapy. *Front Oncol*. 2022;12:985363. doi:10.3389/fonc.2022.985363

92. Wilkinson HN, Hardman MJ. Senescence in Wound Repair: Emerging Strategies to Target Chronic Healing Wounds. *Front Cell Dev Biol*. 2020;8:773. doi:10.3389/fcell.2020.00773

93. Wu YS, Liang S, Li DY, Wen JH, Tang JX, Liu HF. Cell Cycle Dysregulation and Renal Fibrosis. *Front Cell Dev Biol*. 2021;9:714320. doi:10.3389/fcell.2021.714320

94. Rosenwald A, Wright G, Wiestner A, et al. The proliferation gene expression signature is a quantitative integrator of oncogenic events that predicts survival in mantle cell lymphoma. *Cancer Cell*. 2003;3(2):185-197. doi:10.1016/s1535-6108(03)00028-x

95. Naba A, Clauser KR, Ding H, Whittaker CA, Carr SA, Hynes RO. The extracellular matrix: Tools and insights for the "omics" era. *Matrix Biol*. 2016;49:10-24. doi:10.1016/j.matbio.2015.06.003

96. Hynes RO, Naba A. Overview of the Matrisome—An Inventory of Extracellular Matrix Constituents and Functions. *Cold Spring Harb Perspect Biol*. 2012;4(1):a004903. doi:10.1101/cshperspect.a004903

97. Icer MA, Gezmen-Karadag M. The multiple functions and mechanisms of osteopontin. *Clin Biochem*. 2018;59:17-24. doi:10.1016/j.clinbiochem.2018.07.003

98. Sumioka T, Matsumoto K ichi, Reinach PS, Saika S. Tenascins and osteopontin in biological response in cornea. *Ocul Surf*. 2023;29:131-149. doi:10.1016/j.jtos.2023.05.005

99. Miyazaki K ichi, Okada Y, Yamanaka O, et al. Corneal wound healing in an osteopontin-deficient mouse. *Investig Ophthalmol Vis Sci*. 2008;49(4):1367-1375. doi:10.1167/iovs.07-1007

100. Moorman HR, Poschel D, Klement JD, Lu C, Redd PS, Liu K. Osteopontin: A Key Regulator of Tumor Progression and Immunomodulation. *Cancers*. 2020;12(11):3379. doi:10.3390/cancers12113379

101. Saika S, Yamanaka O, Okada Y, Sumioka T. Modulation of Smad signaling by non-TGFβ components in myofibroblast generation during wound healing in corneal stroma. *Exp Eye Res*. 2016;142:40-48. doi:10.1016/j.exer.2014.12.015

102. Varkoly G, Hortobágyi TG, Gebri E, Bencze J, Hortobágyi T, Módis L. Expression Pattern of Tenascin-C, Matrilin-2, and Aggrecan in Diseases Affecting the Corneal Endothelium. *J Clin Med*. 2022;11(20):5991. doi:10.3390/jcm11205991

103. Raghunathan VK, Thomasy SM, Strøm P, et al. Tissue and cellular biomechanics during corneal wound injury and repair. *Acta Biomater*. 2017;58:291-301. doi:10.1016/j.actbio.2017.05.051

104. Dreier B, Thomasy SM, Mendonsa R, Raghunathan VK, Russell P, Murphy CJ. Substratum Compliance Modulates Corneal Fibroblast to Myofibroblast Transformation. *Investig Opthalmology Vis Sci*. 2013;54(8):5901. doi:10.1167/iovs.12-11575

105. Muppala S, Raghunathan VK, Jalilian I, Thomasy S, Murphy CJ. YAP and TAZ are distinct effectors of corneal myofibroblast transformation. *Exp Eye Res*. 2019;180:102-109. doi:10.1016/j.exer.2018.12.009

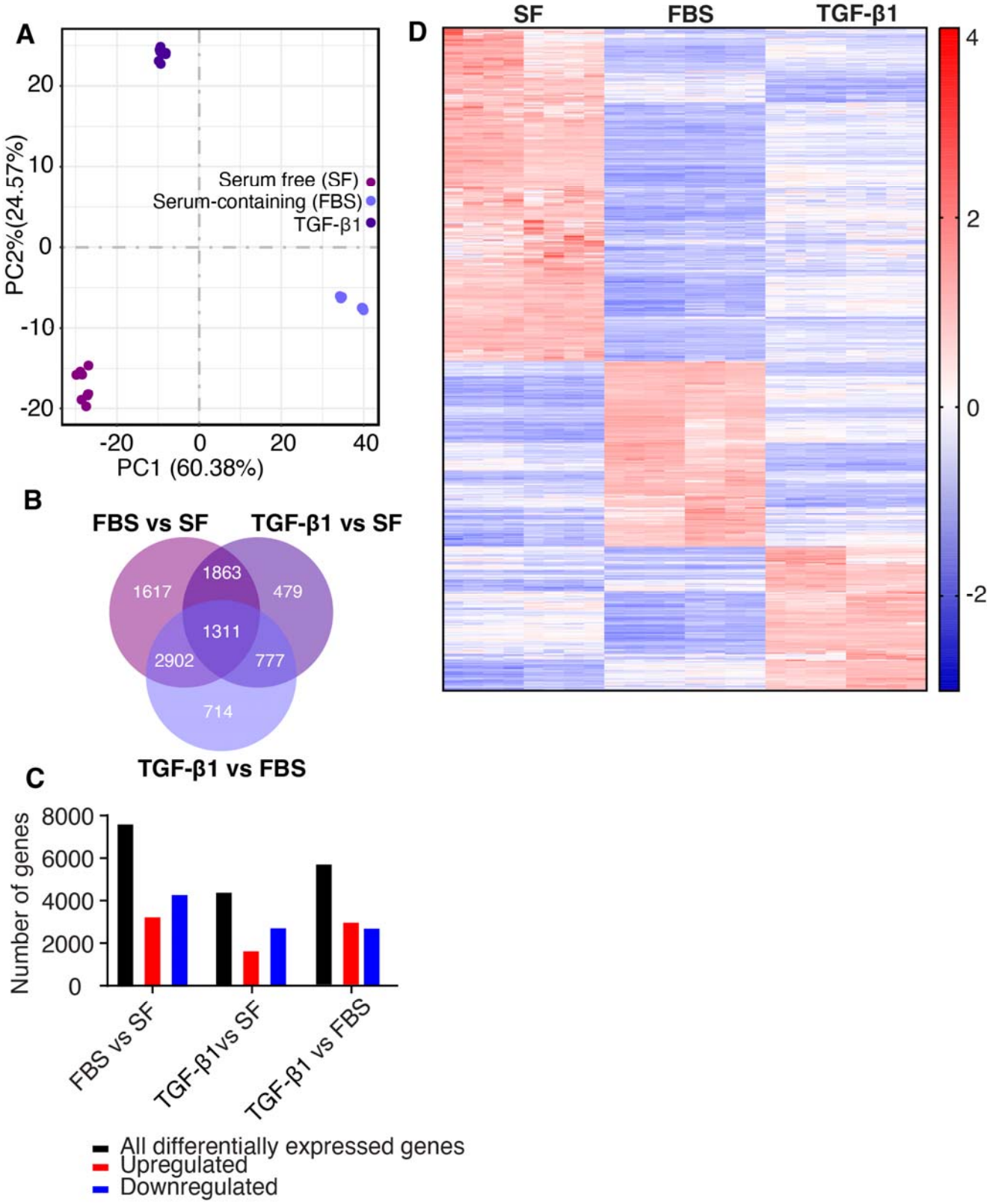
A
PC2%(24.57%)
PC1 (60.38%)
Serum free (SF)
Serum-containing (FBS)
TGF-β1
B
FBS vs SF
TGF-β1 vs SF
TGF-β1 vs FBS
1617
1863
479
1311
2902
777
714
C
Number of genes
FBS vs SF
TGF-β1vs SF
TGF-β1 vs FBS
All differentially expressed genes
Upregulated
Downregulated
D
SF
FBS
TGF-β1

Figure 1. Distinct transcriptional differences exist between cells cultured in the presence of either FBS or TGF-β1. (A) Principal component analysis (PCA) of transcriptional differences between cells cultured in defined serum free (SF) media, FBS or TGF-β1. Principal component (PC) 1 and PC2, account for 60.38% and 24.57% respectively, of the variability among these groups. Analysis was performed using normalized, log2- transformed fragment per kilobase of transcript sequence per million base pairs sequenced (FPKM) values. (B) Venn diagram of differentially expressed genes between groups. (C) Bar plot represents differentially expressed genes either up- or downregulated between different treatment conditions. Gene expression values with an adjusted p-value (padj) < 0.05 and $|\log2(\text{fold change})| \geq 1$ were considered significantly differentially expressed. (D) Heatmap of log2-transformed FPKM values (log2(FPKM+1)) of genes differentially expressed across all three treatment conditions. The values are normalized using the average expression level of the genes across each row. Red color indicates genes with relative high expression levels and blue color indicates genes with lower expression levels.

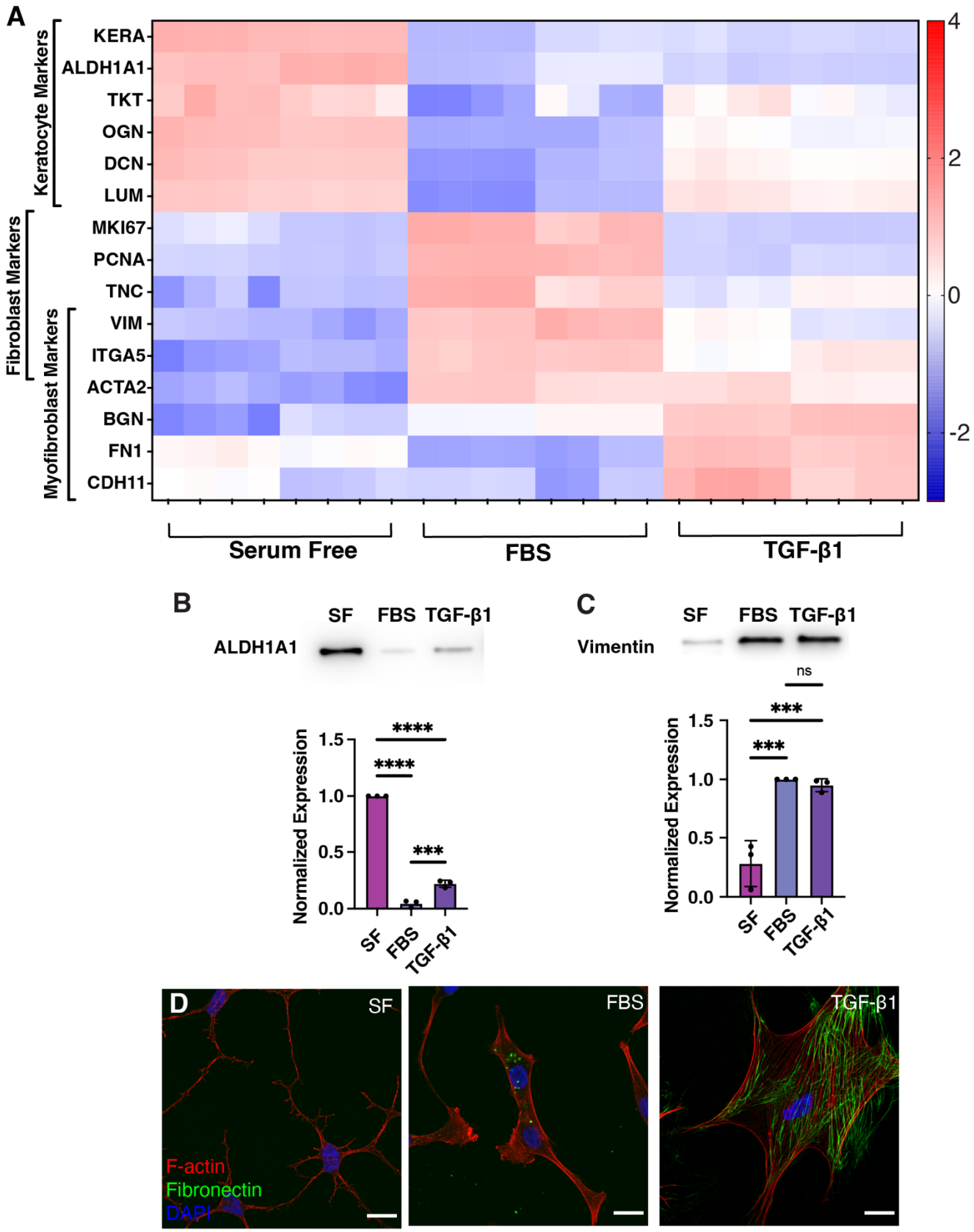

Figure 2. Genes known to be associated with fibroblasts and myofibroblasts are

differentially expressed in the presence of FBS and TGF-β1, respectively. (A) Heatmap indicates the normalized, log2-transformed FPKM values (log2(FPKM+1)) of known quiescent keratocyte, myofibroblast and fibroblast markers. Red color indicates genes with relative high expression levels and blue color indicates genes with lower expression levels. (B, C) Representative western blot and quantification of (B) ALDH1A1 as a marker for keratocytes and (C) Vimentin as a marker for fibroblasts and myofibroblasts. Quantification of protein is normalized to the total protein in each treatment condition. Error bars represent mean ± s.d. for 3 experimental replicates. A one-way ANOVA with a Tukey post-hoc test was used to evaluate significance among groups (*, $p < 0.05$; ****, $p < 0.0001$). (D) Confocal overlay images of fibronectin, phalloidin and DAPI immunofluorescence of corneal keratocytes in serum free (SF) conditions or in the presence of FBS or TGF-β1. Scale bar = 20 µm.

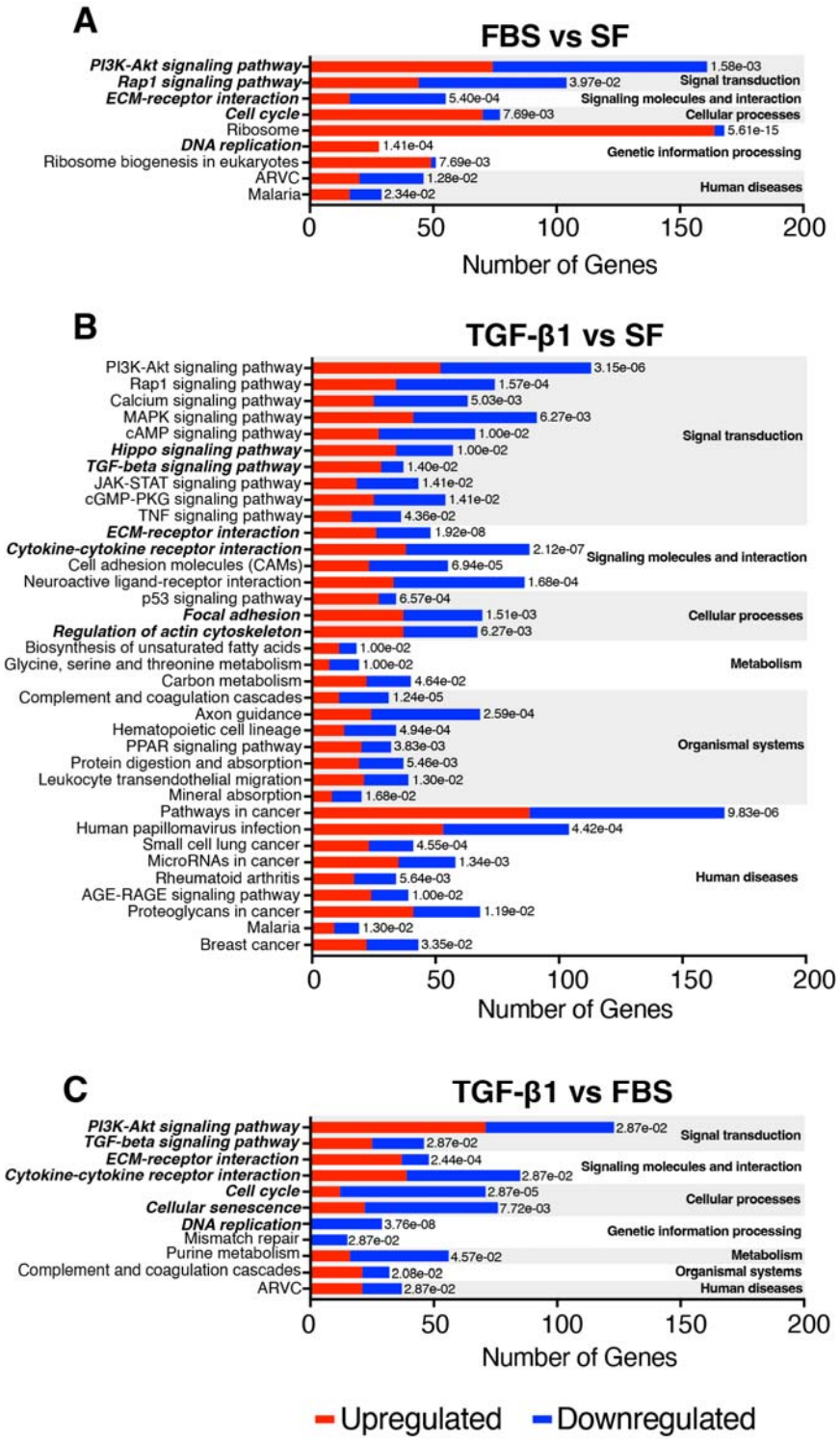

Figure 3. KEGG pathways associated with signal transduction are significantly enriched in the presence of TGF-β1, while pathways associated with genetic

information processing are enriched in the presence of FBS. Bars represent number of genes either up- or downregulated in all the significant KEGG pathways in cells treated with (A) FBS vs. SF (B) TGF-β1 vs. SF (C) TGF-β1 vs. FBS. In each comparison, the alternating grey and white bars differentiate the KEGG pathways grouped together based on their associated function, as indicated on the right corner of each box. Within each group, pathways have been arranged in order of significance, from most to least significant. KEGG pathways with a padj < 0.05 were considered significant. Pathways of particular interest are highlighted in bold type.

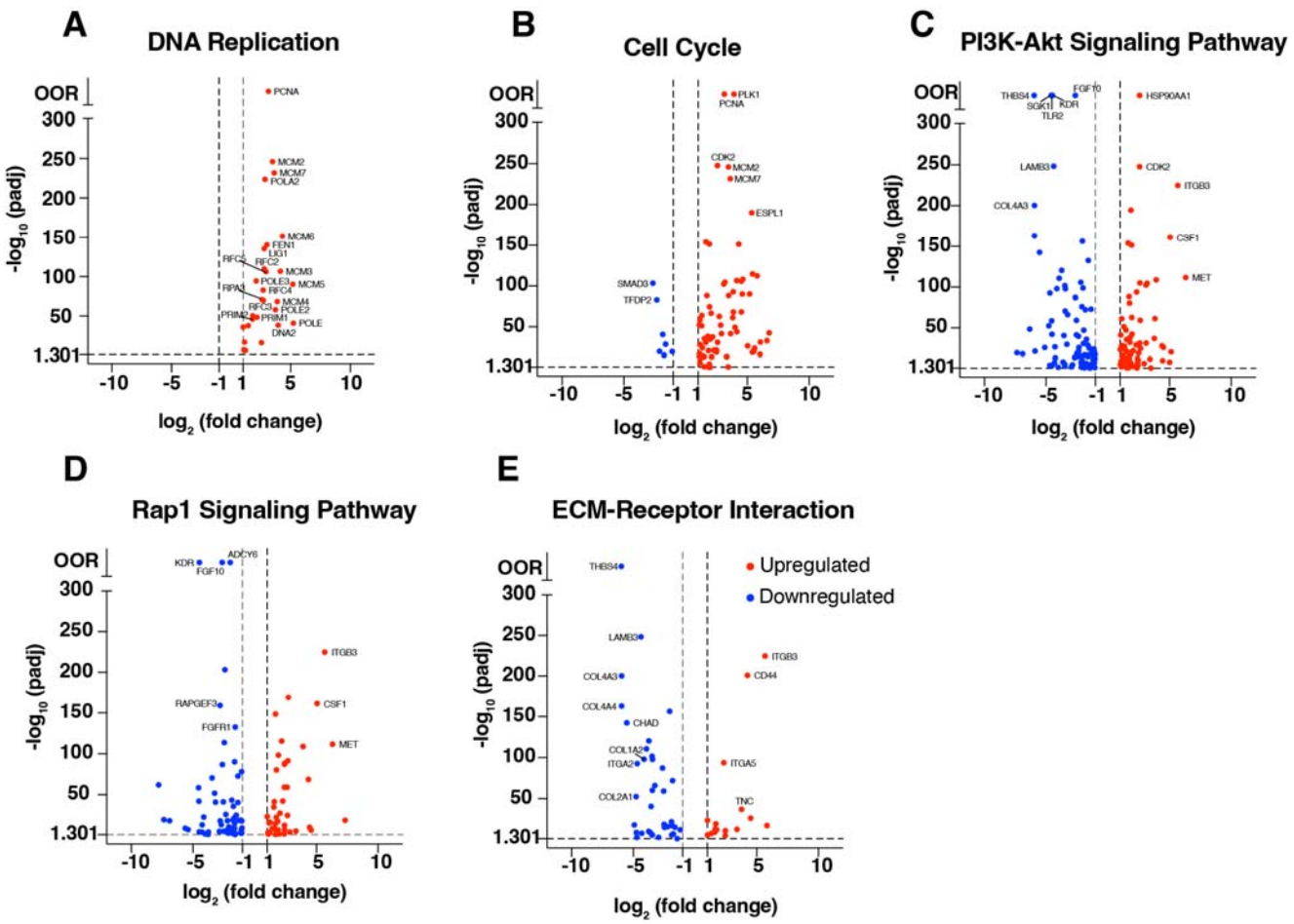

Figure 4. FBS vs. SF: Genes related to a migratory and proliferative phenotype are significantly upregulated in cells cultured in the presence of FBS compared to cells in serum free conditions. (A-E) Volcano plots represent specific genes significantly up- or downregulated in each KEGG pathway, in cells treated with FBS compared to cells in serum free conditions. Genes known to be associated with FBS induced phenotypes and several other significant genes with a high padj value or fold changes have been labeled. Genes with padj < 0.05 (horizontal dashed line) and | log2(fold change) | ≥ 1 (vertical dashed lines) were considered significant. Red dots indicate genes that are upregulated while blue dots indicate downregulated genes.

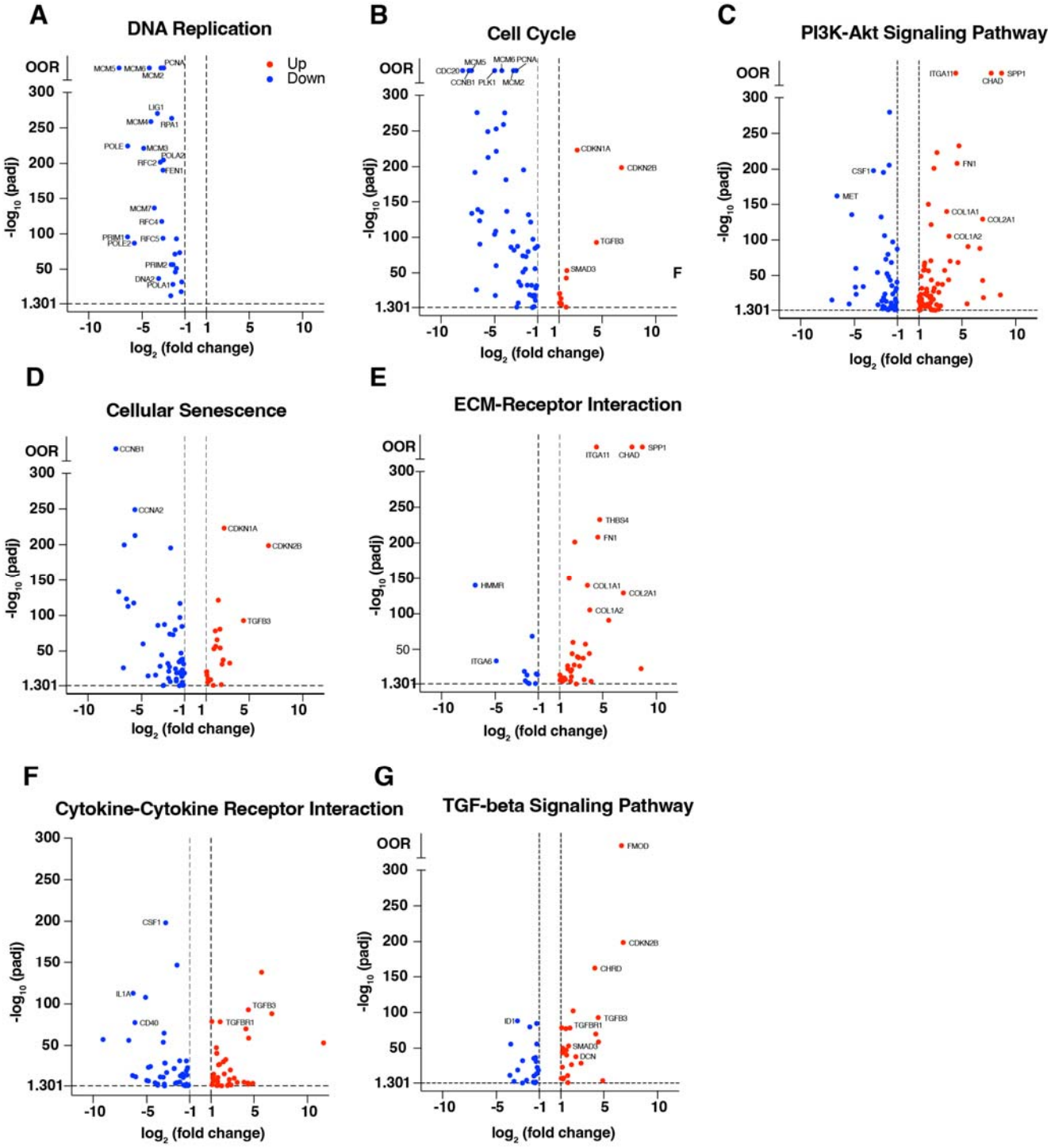
A
DNA Replication
Up
Down
OOR
MCM5
MCM6
PCNA
MCM2
LIG1
MCM4
RPA1
POLE
MCM3
POLA2
RFC2
FEN1
MCM7
RFC4
PRIM1
POLE2
RFC5
PRIM2
DNA2
POLA1
-log10 (padj)
log2 (fold change)
B
Cell Cycle
CDC20
MCM5
MCM6
PCNA
CCNB1
PLK1
MCM2
CDKN1A
CDKN2B
TGFB3
SMAD3
C
PI3K-Akt Signaling Pathway
ITGA11
SPP1
CHAD
CSF1
FN1
MET
COL1A1
COL2A1
COL1A2
D
Cellular Senescence
CCNB1
CCNA2
CDKN1A
CDKN2B
TGFB3
E
ECM-Receptor Interaction
ITGA11
CHAD
SPP1
THBS4
FN1
HMMR
COL1A1
COL2A1
COL1A2
ITGA6
F
Cytokine-Cytokine Receptor Interaction
CSF1
IL1A
CD40
TGFB3
TGFBR1
G
TGF-beta Signaling Pathway
FMOD
CDKN2B
CHRD
ID1
TGFB3
TGFBR1
SMAD3
DCN

Figure 5. TGF-β1 vs. FBS: Proliferation related genes are significantly downregulated, and genes involved in mechanotransduction are upregulated in cells cultured in the presence of TGF-β1 compared to cells in the presence of FBS. (A-G) Volcano plots represent specific genes significantly up- or downregulated in selected KEGG pathways, in cells treated with TGF-β1 compared to cells cultured in FBS. Genes known to be associated with either TGF-β1 or FBS induced phenotypes and several other significant genes with a high padj value or fold changes have been labeled. Genes with padj < 0.05 (horizontal dashed line) and $|\log2(\text{fold change})| \geq 1$ (vertical dashed lines) were considered significant. Red dots indicate genes that are upregulated while blue dots indicate downregulated genes.

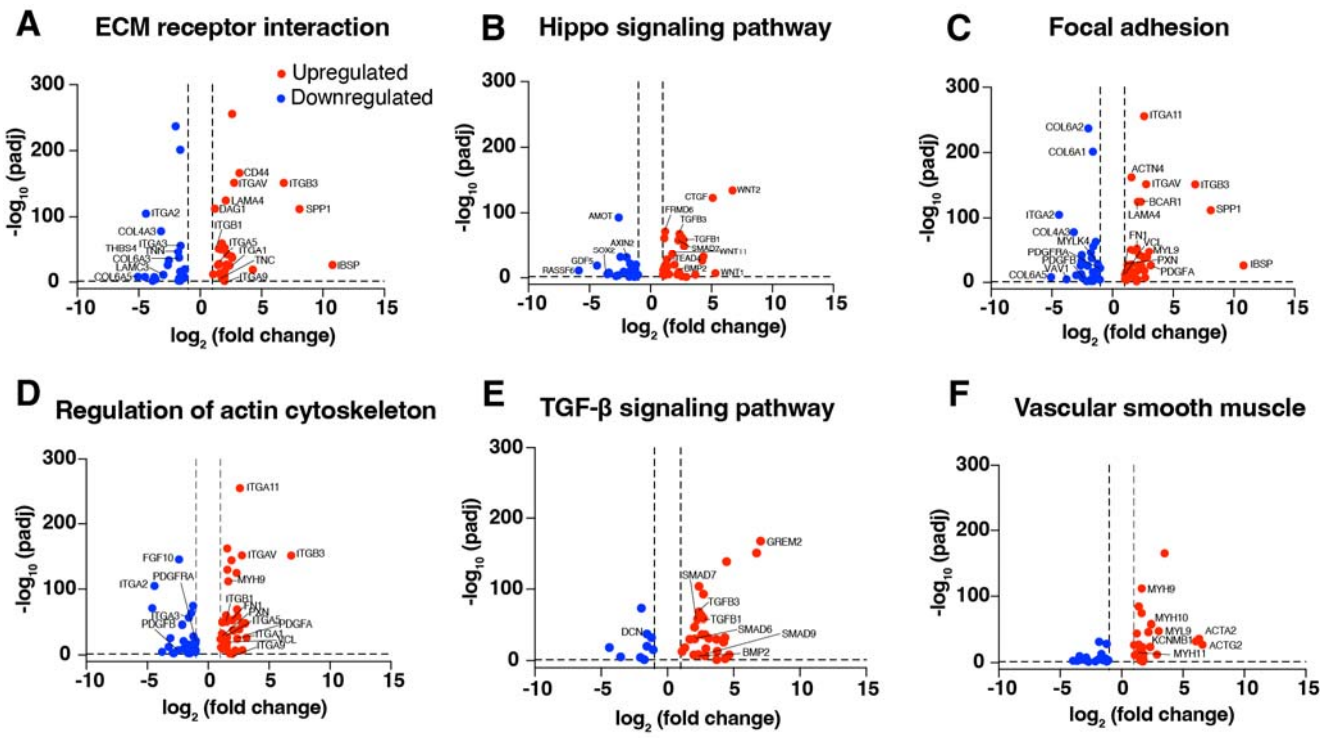

Figure 6. TGF-β1 vs. SF: Several genes in each KEGG pathway related to ECM or mechanotransduction are significantly up- or downregulated in the presence of TGF-β1. (A-F) Volcano plots represent specific genes significantly up- or downregulated in selected KEGG pathways, in cells treated with TGF-β1 compared to cells in serum free conditions. Genes known to be associated with TGF-β1 induced phenotypes and several other significant genes with a high padj value or fold changes have been labeled. Genes with padj < 0.05 (horizontal dashed line) and | log2(fold change) | ≥ 1 (vertical dashed lines) were considered significant. Red dots indicate genes that are upregulated while blue dots indicate downregulated genes.

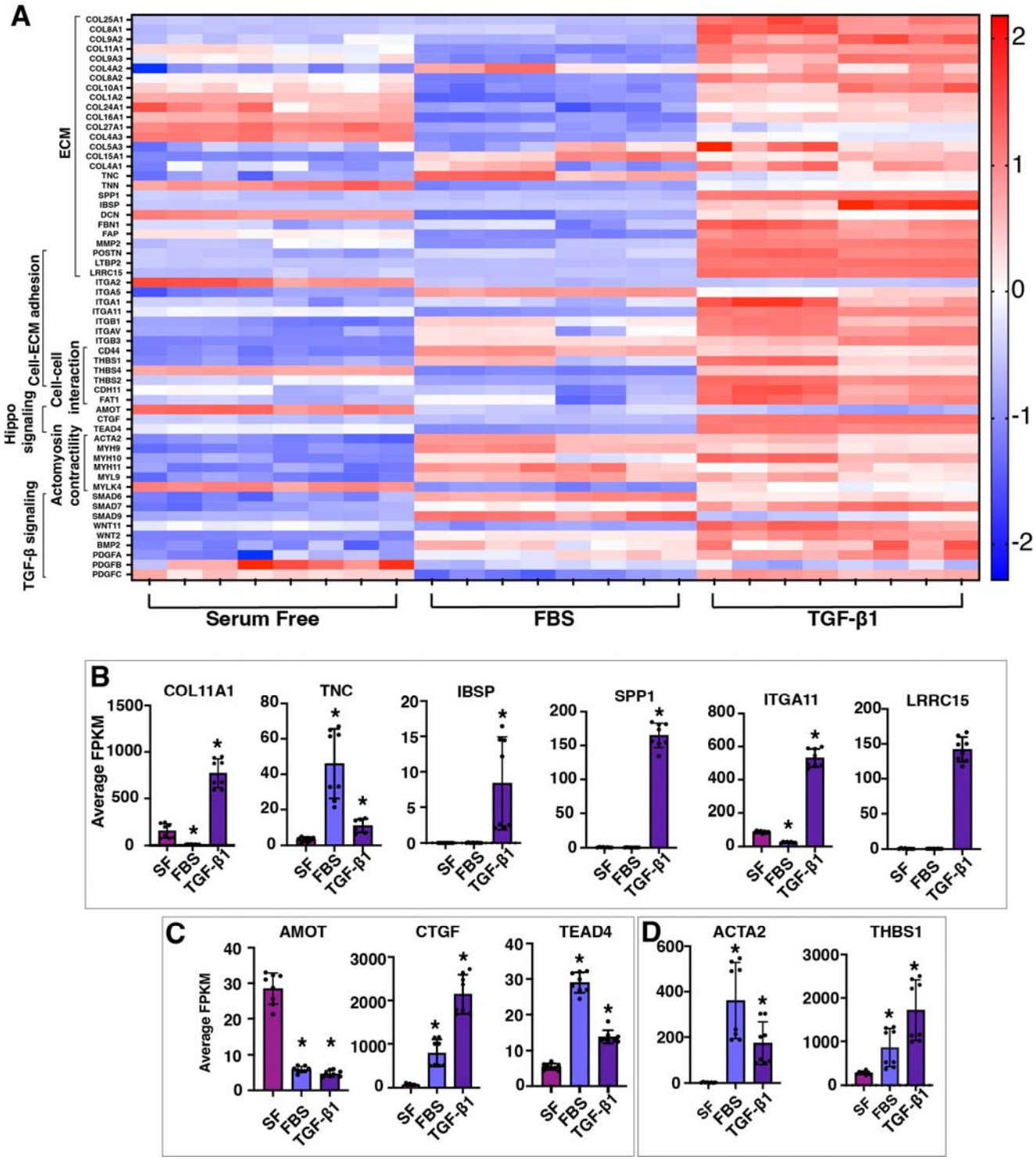

Figure 7. Myofibroblast differentiation is associated with specific ECM and hippo signaling related genes. (A) Heatmap of normalized, log2-transformed FPKM values (log2(FPKM+1)) of several genes associated with ECM, cell-cell interactions and hippo signaling related genes differentially expressed in cells cultured in TGF-β1. Red color indicates genes with relative high expression levels and blue color indicates genes with lower expression levels. Selected genes associated with (B) ECM (C) hippo signaling

and (D) myofibroblast differentiation have been highlighted in the bar graphs. The average FPKM expression values have been indicated for comparison among the three treatment groups. The asterisk denotes a significance level of padj<=0.05 for each treatment condition with respect to serum free conditions.

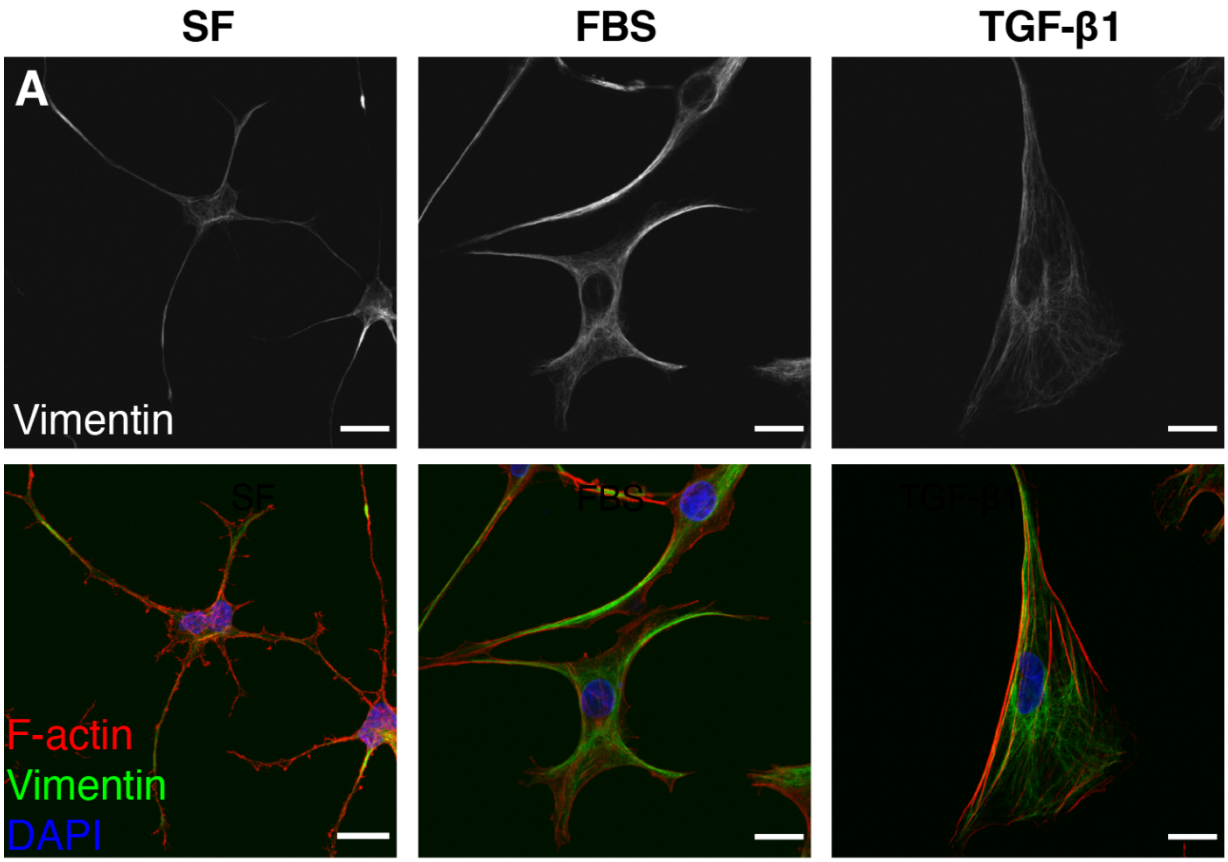

Supplemental figures

Figure S1. Confocal images of (A) vimentin along with (A`) phalloidin and DAPI immunofluorescence of corneal keratocytes in serum free conditions or in the presence of FBS or TGF-β1. Scale bar = 20 µm.

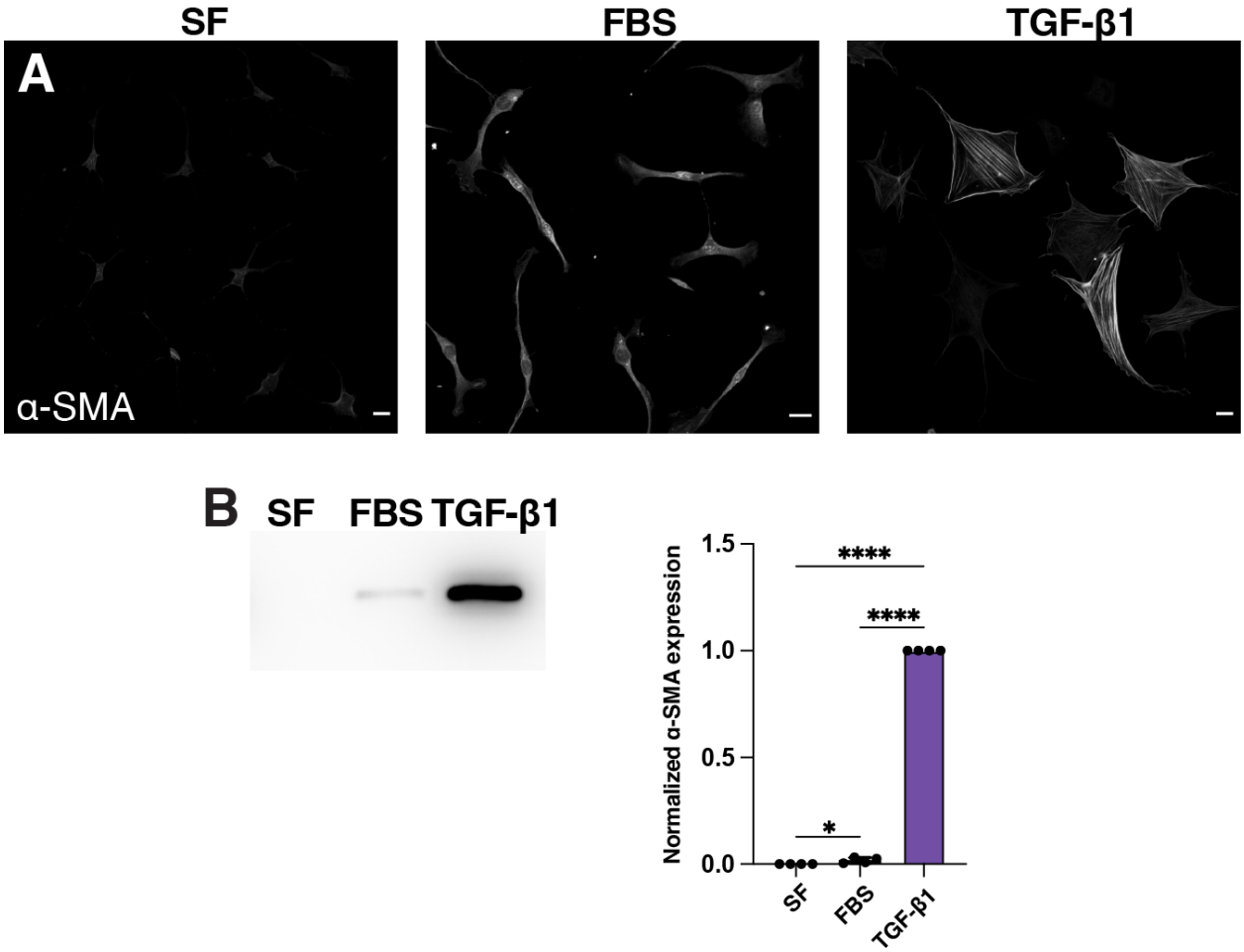

Figure S2. Confocal images of (A) alpha smooth muscle actin (α-SMA) immunofluorescence of corneal keratocytes in serum free conditions or FBS or TGF-β1. Scale bar = 20 µm. (B) Western blot represents α-SMA protein expression levels across treatment conditions. Quantification of protein is normalized to the total protein in each treatment condition. Error bars represent mean ± s.d. for 4 experimental replicates. A one-way ANOVA with a Tukey post-hoc test was used to evaluate significance among groups (*, $p < 0.05$; ****, $p < 0.0001$).

	TGF-β1 vs SF	FBS vs SF
GENES	**padj**	**padj**
COL11A1	6E-17	5.2176E-48
TNC	2.06E-08	9.8924E-38
IBSP	9.64E-27	n.s
SPP1	1.48E-112	n.s
ITGA11	2.34E-256	1.1106E-72
LRRC15	2.97E-78	n.s
AMOT	1.45E-93	3.34E-79
CTGF	9.51E-124	3.41E-42
TEAD4	1.73E-28	3.85E-110
ACTA2	5.52E-37	8.79E-53
THBS1	1.66E-37	6.93E-10

Table S1. Significance values of genes differentially regulated in the presence of FBS or TGF-β1 compared to serum free, represented as padj values. List of genes included are those represented as bar plots in Fig. 7B-D.